Comparative Analysis of Direct Torque Control in Three phase and Five Phase Induction Motor Drives

Saswat Ranjan Mishra

Department of Electrical Engineering

National Institute of Technology Rourkela

Comparative Analysis of Direct Torque Control in Three phase and Five Phase Induction Motor Drives

Thesis submitted in partial fulfillment

of the requirements of the degree of

Master of Technology

in

Electrical Engineering

by

Saswat Ranjan Mishra

(Roll Number: 711EE2162)

based on research carried out

under the supervision of

Prof. Anup Kumar Panda

May, 2016

Department of Electrical Engineering

National Institute of Technology Rourkela

Department of Electrical Engineering
National Institute of Technology Rourkela

May 20, 2016

Supervisor's Certificate

This is to certify that the work presented in the thesis entitled *Comparative analysis of Direct Torque Control in three phase and five phase induction motor drives* submitted by *Saswat Ranjan Mishra*, Roll Number *711EE2162*, is a record of original research carried out by him under my supervision and guidance in partial fulfillment of the requirements of the degree of *Master of Technology* in *Electrical Engineering*. Neither this dissertation nor any part of it has been submitted earlier for any degree or diploma to any institute or university in India or abroad.

Anup Kumar Panda

Professor

Declaration of originality

I, *Saswat Ranjan Mishra*, Roll Number *711EE2162* hereby declare that this thesis entitled *Comparative Analysis of Direct Torque Control in three phase and five phase induction motor drives* presents my original work carried out as a post graduate student of NIT Rourkela and, to the best of my knowledge, contains no material previously published or written by another person, nor any material presented by me for the award of any degree or diploma of NIT Rourkela or any other institution. Works of other authors cited in this thesis have been duly acknowledged under the section "References". I have also submitted my original research records to the scrutiny committee for evaluation of my thesis.

I am fully aware that in case of any non-compliance detected in future, the Senate of NIT Rourkela may withdraw the degree awarded to me on the basis of the present thesis.

May 20, 2016 *Saswat Ranjan Mishra*
NIT Rourkela

ACKNOWLEDGEMENT

On the submission of my thesis on **“Comparative Analysis of Direct Torque Control in three phase and five Phase Induction Motor drives”**, I would like to articulate my deep gratitude and sincere thanks to my supervisor **Prof. Anup Kumar Panda** for his most valuable guidance and thoughtful suggestions during the course of my work throughout the year. His help and advice has been a constant source of inspiration.

I am sincerely thankful to **Prof. Jitendriya Kumar Satapathy ,** Head of the Department, Electrical Engineering and all the faculty members for providing a solid background for my studies and research thereafter. I am thankful to the laboratory staff of the department for their timely help. An assemblage of this nature could never have been attempted without reference to and inspiration from the works of others whose details are mentioned in reference section. I acknowledge my indebtedness to all of them.

I am thankful to all my classmates and the department research scholars for their cooperation and unfailing help during the project work.

I am grateful to all my friends who made my stay in Rourkela, an unforgettable and rewarding experience.

Finally, I feel great reverence for all my family members and the Almighty, for their blessings and for being a constant source of encouragement.

Saswat Ranjan Mishra

Abstract

The Direct Torque Control (DTC) is a type of vector control technique which is used to regulate the torque and hence speed of an induction motor drive. This method is very efficient, cheap and is very easy to execute. The absence of mechanical speed estimators along with the ease of processing and computations make it the most preferred option among all vector control techniques. In this method, only the voltage and current are sensed and they are used to estimate the torque, flux and the angle between the rotor and stator flux. Depending on the torque and flux errors, a suitable voltage vector is selected to keep the errors within the desired tolerance region.

At present times, three phase induction motors have become the backbone of industries. Lifts, agricultural pumps, conveyor belts, lathes, cranes, drilling machine, etc. are some of the prominent areas where induction motors have been very effective. These motors can be controlled using the scalar V/F control techniques. However, for applications requiring quick response vector control techniques like DTC are preferred. But the problem lies in the presence of torque ripples in case of DTC of three phase induction motor drive. Recently it has been seen that multiphase induction machines have the inherent feature of low torque pulsations. Hence they have replaced their three phase counterparts in areas like ship propulsions and aerospace industries where higher accuracy is required. This feature along with many other advantages of multiphase induction machines make them a strong competitor to their three phase counterparts in the field of industrial drives.

This project aims to study and simulate the conventional DTC technique in a five phase induction machine with the help of MATLAB & Simulink and compare the results with its three phase counterpart to verify the effectiveness of the multiphase machine.

Contents

LIST OF SYMBOLS

Subscript:

as, bs, cs : For a, b, c phase respectively

q, d : For q-axis and d-axis respectively

s, r : For stator and rotor respectively

e : Electromagnetic

m : Mutual

l : Leakage

b : Base

Superscript:

s : Stationary

Symbols:

V : Voltage

R : Resistance

i : Current

Ψ : Flux linkage

ω : Angular velocity

F : Product of flux linkage and angular velocity

L : Inductance

T : Torque

P : Number of Poles

X : Reactance

J : Moment of Inertia

σ : Leakage factor

LIST OF FIGURES

LIST OF TABLES

Chapter 1

Introduction

1.1 Overview of Induction Motor

Electrical motors have become an indispensable part of our life with nearly every appliance using some kind of a motor for its functioning. But this all would not have been possible if, Hans Christian Oersted had not discovered the relation between electricity and magnetism. Soon after this discovery, Michael Faraday discovered the effect of concept of electromagnetic rotation and this led to the invention of DC motor. After a few years, Nicola Tesla invented the first AC synchronous motor. For many years these three type of machines were only used until the invention of the induction motor which has now completely taken over as the most preferred motor in the industries.

Due to the ease of the speed control in a DC motor, they were used quite frequently in the industrial purposes. However, with the development of power electronics, currently the switches can be controlled with higher frequency by the help of micro-controllers. This led to the control of magnitude, phase and frequency of the AC supply to the motor and hence could control the speed of the AC motors. However, induction motors are more preferred than other motors because they are easy to construct, have a very rugged construction, have higher efficiency, are more reliable, yet very cheap and are very easy to operate. DC motors have the disadvantage of producing sparks due to commutation failure. As such, they are hazardous to be used in places where there is risk of fire. But the induction motors do not require commutator. Hence there isn't any sparking problems. So they are safe to be used in fire hazardous places. As a result of all these advantages, induction motor is the most preferred motor in industries.

Perfect control of an induction motor is possible only when the frequency as well as the magnitude of the AC supply voltage can be controlled. The speed of the rotating magnetic field of the motor can be controlled by varying the speed. Also the impedance of the motor which is mainly inductive, can vary with varying frequency. Hence to keep the current at safe levels at reduced frequency decreasing the magnitude of voltage is necessary. Conventionally a delta-star transformer was used for this purpose to obtain reduced magnitude of voltages. A change in the pole pair number was also tried but this method was costly and not so efficient.

With the invention of slip ring induction motor and the development of power electronics several speed control theories were proposed:

1. Scalar Control Techniques:

   This method is also called V/F control technique. Here a linear relation is maintained between voltage magnitude and its frequency. This is required to keep the flux at a constant value. If the flux were not maintained constant, then while increasing the speed by increasing the frequency, the flux would have decreased leading to underrating of the motor and while decreasing the speed by decreasing the frequency, the flux would have increased leading to saturation of the core and hence increase in the core loss of the motor. Thus to keep the flux at the rated value, irrespective of the speed change, the V/F ratio is maintained constant. This method is very simple to implement and is widely used to control the speed of the induction motor. However, it gives very sluggish response. This is due to the fact that in an induction motor the torque and flux are not decoupled. For example, when we want to decrease the torque, we need to decrease the slip and hence decreasing the frequency. But, this leads to an increase in the flux. Similar case happens while trying to increase the speed, where there is a decrease in flux. Moreover, the control loop for flux is also sluggish and this leads to the time of response getting enhanced.
2. Vector control technique:

   To solve the problem of the sluggish response of the scalar control methods, vector control methods were proposed in the 1970s. They solve the problem of inherent coupling of torque and flux in induction machines. These methods provide a dc motor type control where the torque and flux are decoupled. Using Clarke and Park transformations the sinusoidal quantities in an induction machine can be transformed to dc quantities. The controlling currents can be resolved into two mutually perpendicular currents which separately control the torque and flux just like in a dc motor. This method gives very good dynamic response but needs complex programming and implementation.
3. Direct Torque Control Technique:

   Takahashi and Dopenbrock first introduced this method which has now become the easiest and yet the best method for speed and torque control of an induction motor.

This method doesn't require any current control loops, any rotor position measuring device or any complex coordinate transformations. The use of hysteresis band controllers, keep the flux and torque within preferred limits. This method is best for applications requiring quick torque response.

Advantages of DTC [20]:

- By varying the torque and flux reference the corresponding outputs can be changed very fast.
- It has higher efficiency because of low switching losses. The semiconductor switches are switched only to when it is required to keep the values of torque and flux within the hysteresis band.
- No coordinate transformations are needed as the calculations are done in the stationary reference frame.
- No current control loops are required. This reduces the problem of tuning of current controllers.
- It has fast torque response.

Disadvantages of DTC:

- The switching frequency of the switches is not constant. However, by providing suitable hysteresis bands the average switching frequency can be matched with the reference value.
- Torque and flux estimators are required.

Comparison between DTC and FOC:

1. The dynamic response to torque changes is very fast in DTC compared to FOC.
2. The reference frame used in DTC is the stationary reference frame (alpha, beta) compared to rotating reference frame (d-q) in FOC.
3. The variables that are controlled in DTC are torque and flux linkage. In FOC, the variables that are controlled are rotor flux, torque current component i_q and flux current component i_d.
4. The torque ripple is higher in DTC than FOC. This is due to the presence of hysteresis controllers in DTC.
5. The exact position of rotor is not required to measure in case of DTC but in FOC the rotor position measurement is required. Hence Hall effect sensors are used.

6. As the control variables include current components in FOC, current controlling loops are required in FOC but these are absent in DTC. This leads to complexity in tuning problems in case of FOC.
7. PWM modulator is required in FOC but not in DTC.
8. As DTC uses stationary frame of reference, transformations to complex rotating frame is not required. But this is required in FOC.
9. Due to uneven switching pulses, the switching frequency is not constant in case of DTC. But it is constant in case of FOC.
10. Due to the use of hysteresis controller, the switching losses are lower in case of DTC.
11. The complexity in programming and calculations is higher in case of FOC.

Though three phase induction motors are predominantly used in all industrial purposes, if the supply is provided through an inverter, there is no restriction on the number of phases. A lot of papers have been published which have established the fact that machines with higher number of phases are more advantageous than their three phase counterparts.

A few advantages are [22]:

1. The efficiency in a multi-phase machine is higher than the three phase machine because of low value of space harmonic components produced by stator field excitation.
2. The tolerance to fault is higher in multi-phase machines. This is because if one phase of a three phase machine is exposed to fault, the machine can work as a single phase machine but will need external support for starting and also there will be derating of the motor. However, in a multi-phase machine there would not be any starting problems as the machine can start by itself and the derating will also be very less.
3. The multi-phase machines have higher tolerance to time harmonic contents due to excitation of stator field than the three phase machines. These time harmonic excitation contents can generate torque pulsations with frequency of the order of even multiples of source frequency.
4. The power rating of the components used to drive the multi-phase machine is less compared to the three phase machine for the same amount of power output.

As a result of these advantages, certain applications like aerospace, ship propulsion and hybrid vehicles have already started using multi-phase machine as an alternative to three phase machines.

1.2 Literature survey

In 1986 Takahashi and Noguchi [1] gave an idea about a new control strategy called Direct Torque Control which uses an optimum voltage vector to regulate the torque and flux. The objective was to obtain very fast torque response with lower switching frequency and lower harmonic losses. The efficiency obtained in this method was also high. This employed a standard look up table to select the proper switching vector.

In 1988 Depenbrock [2] removed the unnecessary requirement of mechanical speed measurement for inverter –fed induction machines. He proposed a method to calculate accurately the motor speed without mechanical devices using Direct Self Control (DSC) strategies.

In 1992 Thomas G. Habetler [3] proposed the method of Space Vector modulation technique for Direct Torque Control. In this method a voltage vector was calculated in a dead beat fashion so as to control the torque and flux directly. Using the space vector PWM technique, the duty cycle of the inverter can then be calculated. The advantage of this scheme is that the current loops and the PI controllers are no longer needed.

In 1995 Mir and Elbuluk [4] proposed the fuzzy logic approach to determine the appropriate switching vectors in the DTC scheme. The construction and topology remains similar as that of the conventional DTC. In the conventional method, the switching vector remained on for the entire switching period. This produced significant ripples. However in this paper it was shown that by using switching vectors only for a fraction of the switching period and using the null vectors for the rest of the period reduced the ripples. This is also called duty ratio control.

In 1999 Chen and Li [5] proposed a scheme to reduce the torque ripples and improve the locus of the flux at low speeds. This method is called predictive control scheme. A constant and larger switching frequency is generated by using the virtual vector concept. Wider bandwidth speed control is achieved in this method. The precision at steady state is good and the response to dynamic torque is also improved.

In 1999 Telford, Dunnigan and Williams [6] proposed a duty cycle scheme of control which makes the average torque equal to the minimum hysteresis limit with the help of duty cycle controller. The non-linear effects of DTC is also analyzed. The importance of this paper is that the essence of DTC, that is its simplicity is not eroded.

In 1999 Kang and Sul [7] proposed a method to reduce the torque ripple in DTC by maintain the switching frequency constant. In this method, by using the instantaneous torque equations a rms torque-ripple equation was developed. Using the torque ripple equation an optimum switching instant is determined in each switching cycle which satisfies the criteria for minimum torque ripple. The performance of DTC is improved in this method.

In 2001 Lin and Fang [8] proposed the sliding mode DTC scheme. Two sliding surfaces are designed for the torque and flux separately to establish DTC. Here integral sliding surface is used for torque and the Benchaib model is used for flux sliding surface.

In 2005 Yourui and Chaoli [9] proposed a method to implement the general mapping regressor neural network to the DTC scheme. In this method the neural network is self organized and contains a large chain of neurons.

In 2015 Dybkowski and Szabat [10] proposed a method of adaptive compensator which is based on the structure of MRAC. The fuzzy logic is implemented here with the facility of online tuning of the desired parameter. The weights of the controller are tuned online according to the error obtained. This improved the performance of the drive for varying conditions.

In 2016 Alsofyani and Idris [11] proposed a method to obtain torque and flux estimates in very low speeds. In this the three level torque hysteresis controller is replaced by a constant switching frequency controller. This is called DTC-CSFC. By the help of extended Kalman filter the speed feedback is measured. Hence this needs very heavy computation. But the sampling time is small and bandwidth is large due to the simple structure.

In 1991 Toliyat etal. [12] presented the analysis of the performance and features of multiphase concentrated windings which are designed to be operated with static power electronic converters. The equations related to the transient and steady state performance of the machine was derived. Some equations related to voltage and torque were modified due to non-sinusoidal flux distribution.

In 1969 Ward and Harer [13] performed a series of experiments on inverter fed five phase induction motor and presented their observations. They concluded that the current and torque output for a five phase motor is the dual analogue of its three phase counterpart. The torque pulsations achieved in case of a five phase motor is one third of that obtained in a three phase machine.

In 1983 Klingshrin [14] performed a series of experiments on high phase order (HPO) induction motors to study their characteristics. He concluded that these HPO motors can start and run even if one of their phase is open. If the number of phases are more the derating is significantly less. When sinusoidal supply is given, their performance is identical to three phase motors but with non sinusoidal supply the performance varies. The stator copper loss due to harmonics is more but the rotor copper loss and torque pulsations are less. Some space harmonics are removed and hence the stray load loss are less.

In 1988 [15] Pavithran etal. studied the inverter fed five phase induction motor drives. They concluded that in high power applications the five phase drive can be a suitable option, specially in areas like space vehicles and remotely controlled drives where reliability is the highest priority. It was shown that these are more reliable as they are more tolerant to faults.

In 2001 [16] Toliyat and Xu presented a method for the conventional DTC scheme in a five phase Induction motor. They presented the state vector diagram and the effects of the switching vectors. The torque and current waveforms were obtained and compared with that of a three phase machine and it was concluded that the five phase machine gives lesser torque pulsations.

In 2006 Lu, Corzine [17] proposed DTC in a five phase induction machine using space vector modulation techniques. The distortion in current due to the absence of back EMF is analyzed for certain harmonics. They have mainly addressed two drawbacks of the conventional DTC scheme. One is the higher torque pulsation and the other is absence of back EMF for certain low frequency harmonic components which donot produce torque.

In 2011 Khaldi [18] proposed a sensorless method for DTC in a five phase induction motor. In this method the speed is estimated through the power measurement. The scheme was tested under varying load conditions and implemented in real time also. The method used only ten large vectors to get very fast dynamics.

In 2012 Riveros [19] presented a paper to analyze the common mode voltage and proposed tw DTC schemes which used low CMV. It was also proposed to eliminate certain switching states to achieve better torque and flux response and lower peak to peak Common mode voltage. However, there was a small increase in the current distortion.

1.3 Motivation

Direct Torque Control has been the best method to control the speed and torque of three phase induction motors. However, the only flaw is its significant torque ripple. Multi-phase induction machines provide a lot of advantages over their three phase counterpart one of them being lower torque pulsations. The objective of the project is to make use of both these facts i.e. to implement the conventional DTC scheme on a multi-phase induction machine so as to achieve significantly lower torque ripples and compare the results with those obtained with a three phase induction machine. For simplicity, a five phase induction machine is taken as the multi-phase machine.

1.4 Objective

The objective of the project is to simulate DTC on both three phase and five phase induction motor and compare the torque response in both cases. Though the three phase machine has a lot of advantages, it produces significant ripples when DTC is performed on it. The aim here is to verify that a five phase induction motor produces lesser torque ripples than its three phase counterpart.

1.5 Overview of the thesis

Chapter 2: It explains the concept of Direct Torque Control along with its detailed process. It gives an idea about the hysteresis controllers. Axes transformation of three phase voltage vectors is explained in this section and the equation for state space vector is obtained. The three phase induction motor is modelled and the Simulink model is presented.

Chapter 3: It describes the theory of three phase voltage source inverter. The eight switching states in a three phase VSI are discussed along with the state vector diagram. The impact of each state vector on the torque and flux of the IM is examined and an optimum look up table is prepared. Simulink model for the DTC block is presented.

Chapter 4: It explains the axes transformation of five phase voltage vectors and gives an idea about modelling a five phase induction machine. Five phase VSI is described and its thirty-two switching states are studied. The state vector diagram is shown to get an idea about the three vector groups. The effect of each vector group is illustrated. An optimum look up table is prepared and the Simulink model for the DTC block is presented.

Chapter 5: DTC is performed by MATLAB/Simulink for both three phase and five phase IM. The waveforms for torque ripple and stator currents are obtained. Also a plot between rotor and stator flux linkage is obtained. The results obtained from both the machines are compared.

Chapter 6: The summary of the work done is presented along with the conclusion and directions for future work.

Chapter 2

General Theory of Induction Motor and DTC

Induction motors can be controlled by both scalar as well as vector control. However, due to the sluggish response in case of scalar control techniques, the use of vector control is more preferred where fast and dynamic torque response is required. The main reason of the sluggish response obtained in case of scalar control is the coupled nature of torque and flux. However, in vector control the torque and flux are aligned along two mutually perpendicular axes, i.e. they are orthogonal or decoupled quantities. Hence axes transformation from three phase quantities to two mutually perpendicular quantities is the fundamental of vector control.

2.1 Axes transformation

Let us consider a symmetrical three phase induction machine with stationary a-b-c axes at $\frac{2\pi}{3}$ angle apart as shown in Figure 1.1. We have to transform the three phase stationary reference frame variables into the two phase stationary reference frame ($d^s - q^s$) variables.

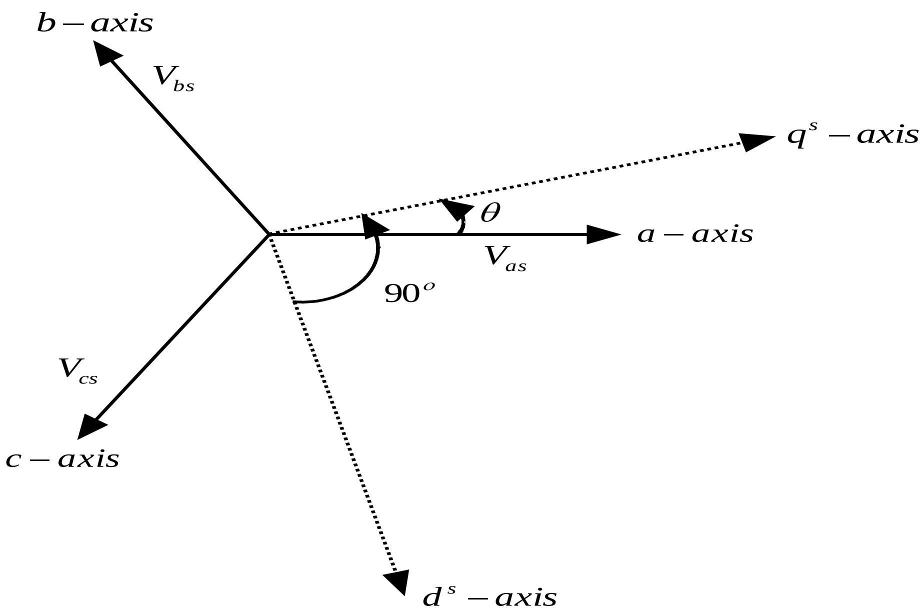

Figure 1.1: Transformation from a-b-c axis to $d^s - q^s$ axes

Let us assume that $d^s - q^s$ axes are oriented at θ angle. Now resolving the two voltage vectors ${V_{qs}}^s and\ {V_{ds}}^s$ we have,

$$V_{as} = {V_{qs}}^s \cos\theta + {V_{ds}}^s \sin\theta \qquad \cdots\cdots\cdots (2.1)$$

$$V_{bs} = {V_{qs}}^s \cos(\theta - 120°) + {V_{ds}}^s \sin(\theta - 120°) \qquad \cdots\cdots\cdots (2.2)$$

$$V_{cs} = {V_{qs}}^s \cos(\theta + 120°) + {V_{ds}}^s \sin(\theta + 120°) \qquad \cdots\cdots\cdots (2.3)$$

So,

$$\begin{bmatrix} V_{as} \\ V_{bs} \\ V_{cs} \end{bmatrix} = \begin{bmatrix} \cos\theta & \sin\theta & 1 \\ \cos(\theta - 120°) & \sin(\theta - 120°) & 1 \\ \cos(\theta + 120°) & \sin(\theta + 120°) & 1 \end{bmatrix} \begin{bmatrix} {V_{qs}}^s \\ {V_{ds}}^s \\ {V_{0s}}^s \end{bmatrix} \qquad \cdots\cdots\cdots (2.4)$$

Where ${V_{0s}}^s$ is added as the zero sequence current component which may or may not be present.

Taking inverse of the matrix we get,

$$\begin{bmatrix} {V_{qs}}^s \\ {V_{ds}}^s \\ {V_{0s}}^s \end{bmatrix} = \frac{2}{3} \begin{bmatrix} \cos\theta & \cos(\theta - 120°) & \cos(\theta + 120°) \\ \sin\theta & \sin(\theta - 120°) & \sin(\theta + 120°) \\ 1/2 & 1/2 & 1/2 \end{bmatrix} \begin{bmatrix} V_{as} \\ V_{bs} \\ V_{cs} \end{bmatrix} \qquad \cdots\cdots\cdots (2.5)$$

If we assume $\theta = 0°$, and ignoring the zero sequence component,

$$\begin{bmatrix} {V_{qs}}^s \\ {V_{ds}}^s \end{bmatrix} = \frac{2}{3} \begin{bmatrix} 1 & \cos(-120°) & \cos(+120°) \\ 0 & \sin(-120°) & \sin(+120°) \end{bmatrix} \begin{bmatrix} V_{as} \\ V_{bs} \\ V_{cs} \end{bmatrix} \qquad \cdots\cdots\cdots (2.6)$$

In the complex form we can write,

$$\overrightarrow{V_s} = {V_{qs}}^s - j{V_{ds}}^s$$

⇨ $\overrightarrow{V_s} = \frac{2}{3}[V_{as}(1 - j0) + V_{bs}(\cos(-120°) - j\sin(-120°)) + V_{cs}(\cos(120°) - j\sin(120°))]$

⇨ $\overrightarrow{V_s} = \frac{2}{3}[V_{as} + V_{bs}(\cos(120°) + j\sin(120°)) + V_{cs}(\cos(-120°) + j\sin(-120°))]$

⇨ $\overrightarrow{V_s} = \frac{2}{3}\left[V_{as} + V_{bs}e^{i2\pi/3} + V_{cs}e^{-i2\pi/3}\right] \qquad \cdots\cdots\cdots (2.7)$

2.2 Modelling of a three phase induction motor

The stator circuit equations can be written as

$$V_{qs}{}^{s} = R_s i_{qs}{}^{s} + \frac{d}{dt}\Psi_{qs}{}^{s} \qquad \cdots\cdots\cdots (2.8)$$

$$V_{ds}{}^{s} = R_s i_{ds}{}^{s} + \frac{d}{dt}\Psi_{ds}{}^{s} \qquad \cdots\cdots\cdots (2.9)$$

Where $\Psi_{qs}{}^{s}$ and $\Psi_{ds}{}^{s}$ are q-axis and d-axis stator flux linkages respectively.

On converting to d-q frame, we have

$$V_{qs} = R_s i_{qs} + \frac{d}{dt}\Psi_{qs} + \omega_e \Psi_{ds} \qquad \cdots\cdots\cdots (2.10)$$

$$V_{ds} = R_s i_{ds} + \frac{d}{dt}\Psi_{ds} - \omega_e \Psi_{qs} \qquad \cdots\cdots\cdots (2.11)$$

The last two terms are speed emf due to rotation of the axes.

The rotor equations are

$$V_{qr} = R_r i_{qr} + \frac{d}{dt}\Psi_{qr} + (\omega_e - \omega_r)\Psi_{dr} \qquad \cdots\cdots\cdots (2.12)$$

$$V_{dr} = R_r i_{dr} + \frac{d}{dt}\Psi_{dr} - (\omega_e - \omega_r)\Psi_{qr} \qquad \cdots\cdots\cdots (2.13)$$

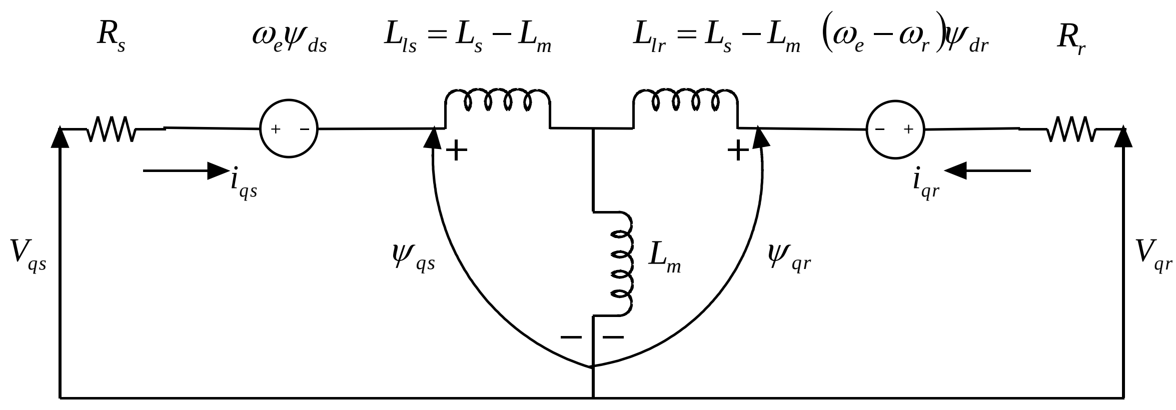

Figure 1.2: q-axis phase equivalent circuit of induction motor

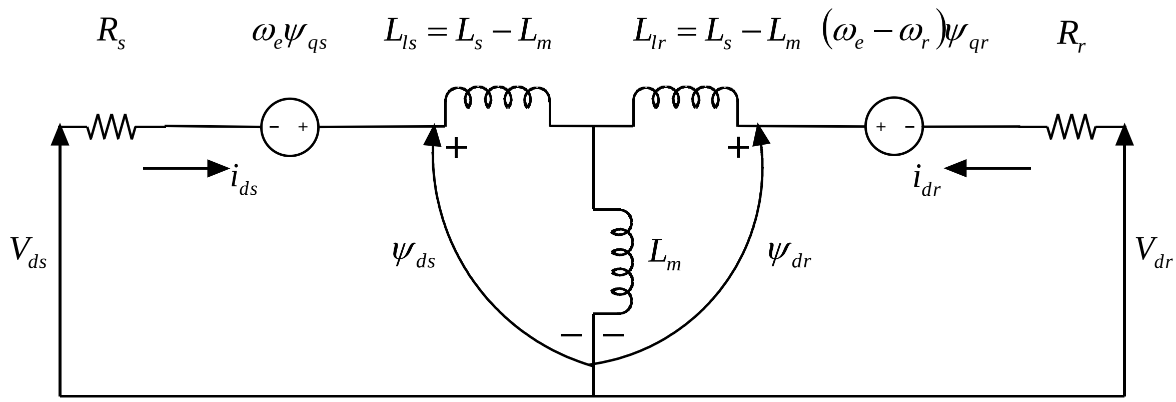

Figure 1.3: d-axis phase equivalent circuit of induction motor

The flux linkage expressions in terms of currents can be written as

$$\Psi_{qs} = L_{ls}i_{qs} + L_m(i_{qs} + i_{qr}) \qquad \cdots\cdots\cdots (2.14)$$

$$\Psi_{qr} = L_{lr}i_{qr} + L_m(i_{qs} + i_{qr}) \qquad \cdots\cdots\cdots (2.15)$$

$$\Psi_{qm} = L_m(i_{qs} + i_{qr}) \qquad \cdots\cdots\cdots (2.16)$$

$$\Psi_{ds} = L_{ls}i_{ds} + L_m(i_{ds} + i_{dr}) \qquad \cdots\cdots\cdots (2.17)$$

$$\Psi_{dr} = L_{lr}i_{dr} + L_m(i_{ds} + i_{dr}) \qquad \cdots\cdots\cdots (2.18)$$

$$\Psi_{dm} = L_m(i_{ds} + i_{dr}) \qquad \cdots\cdots\cdots (2.19)$$

So in matrix form we have

$$\begin{bmatrix} V_{qs} \\ V_{ds} \\ V_{qr} \\ V_{dr} \end{bmatrix} = \begin{bmatrix} R_s + sL_s & \omega_e L_s & sL_m & \omega_e L_m \\ -\omega_e L_s & R_s + sL_s & -\omega_e L_m & sL_m \\ sL_m & (\omega_e - \omega_r)L_m & R_r + sL_r & (\omega_e - \omega_r)L_r \\ -(\omega_e - \omega_r)L_m & sL_m & -(\omega_e - \omega_r)L_r & R_r + sL_r \end{bmatrix} \begin{bmatrix} i_{qs} \\ i_{ds} \\ i_{qr} \\ i_{dr} \end{bmatrix} \qquad \cdots\cdots\cdots (2.20)$$

Here $L_s = L_{ls} + L_m$ and $L_r = L_{lr} + L_m$, s is the Laplacian operator

The Torque can be generally expressed as

$$T_e = \frac{3}{2}\left(\frac{P}{2}\right)\overrightarrow{\Psi_m} \times \overrightarrow{I_r} \qquad \cdots\cdots\cdots (2.21)$$

Resolving $\overrightarrow{\Psi_m}$ and $\overrightarrow{I_r}$ into d-q components we have,

$$T_e = \frac{3}{2}\left(\frac{P}{2}\right)(\Psi_{dm}i_{qr} - \Psi_{qm}i_{dr}) \qquad \cdots\cdots\cdots (2.22)$$

This can be written in other forms such as

$$T_e = \frac{3}{2}\left(\frac{P}{2}\right)\left(\Psi_{dm}i_{qs} - \Psi_{qm}i_{ds}\right) \qquad \cdots\cdots\cdots (2.23)$$

$$T_e = \frac{3}{2}\left(\frac{P}{2}\right)\left(\Psi_{ds}i_{qs} - \Psi_{qs}i_{ds}\right) \qquad \cdots\cdots\cdots (2.24)$$

$$T_e = \frac{3}{2}\left(\frac{P}{2}\right)L_m\left(i_{qs}i_{dr} - i_{ds}i_{qr}\right) \qquad \cdots\cdots\cdots (2.25)$$

$$T_e = \frac{3}{2}\left(\frac{P}{2}\right)\left(\Psi_{dr}i_{qr} - \Psi_{qr}i_{dr}\right) \qquad \cdots\cdots\cdots (2.26)$$

In stationary frame, taking $\omega_e = 0$ and $V_{qr} = V_{dr} = 0$, we have

$$V_{qs}{}^{s} = R_s i_{qs}{}^{s} + \frac{d}{dt}\Psi_{qs}{}^{s} \qquad \cdots\cdots\cdots (2.27)$$

$$V_{ds}{}^{s} = R_s i_{ds}{}^{s} + \frac{d}{dt}\Psi_{ds}{}^{s} \qquad \cdots\cdots\cdots (2.28)$$

$$0 = R_r i_{qr}{}^{s} + \frac{d}{dt}\Psi_{qr}{}^{s} - \omega_r \Psi_{dr}{}^{s} \qquad \cdots\cdots\cdots (2.29)$$

$$0 = R_r i_{dr}{}^{s} + \frac{d}{dt}\Psi_{dr}{}^{s} + \omega_r \Psi_{qr}{}^{s} \qquad \cdots\cdots\cdots (2.30)$$

Similarly, the torque equations can also be written

$$T_e = \frac{3}{2}\left(\frac{P}{2}\right)\left(\Psi_{dm}{}^{s}i_{qr}{}^{s} - \Psi_{qm}{}^{s}i_{dr}{}^{s}\right) \qquad \cdots\cdots\cdots (2.31)$$

$$T_e = \frac{3}{2}\left(\frac{P}{2}\right)\left(\Psi_{dm}{}^{s}i_{qs}{}^{s} - \Psi_{qm}{}^{s}i_{ds}{}^{s}\right) \qquad \cdots\cdots\cdots (2.32)$$

$$T_e = \frac{3}{2}\left(\frac{P}{2}\right)\left(\Psi_{ds}{}^{s}i_{qs}{}^{s} - \Psi_{qs}{}^{s}i_{ds}{}^{s}\right) \qquad \cdots\cdots\cdots (2.33)$$

$$T_e = \frac{3}{2}\left(\frac{P}{2}\right)L_m\left(i_{qs}{}^{s}i_{dr}{}^{s} - i_{ds}{}^{s}i_{qr}{}^{s}\right) \qquad \cdots\cdots\cdots (2.34)$$

$$T_e = \frac{3}{2}\left(\frac{P}{2}\right)\left(\Psi_{dr}{}^{s}i_{qr}{}^{s} - \Psi_{qr}{}^{s}i_{dr}{}^{s}\right) \qquad \cdots\cdots\cdots (2.35)$$

Dynamic Model

Let us define the flux linkage variables as follows:

$$F_{qs} = \omega_b \Psi_{qs} \qquad \cdots\cdots\cdots (2.36)$$

$$F_{qr} = \omega_b \Psi_{qr} \qquad \cdots\cdots\cdots (2.37)$$

$$F_{ds} = \omega_b \Psi_{ds} \qquad \cdots\cdots\cdots (2.38)$$

$$F_{dr} = \omega_b \Psi_{dr} \quad \cdots\cdots\cdots (2.39)$$

Where, ω_b = base frequency of the machine

Substituting we have

$$V_{qs} = R_s i_{qs} + \frac{1}{\omega_b}\left(\frac{d}{dt}F_{qs} + \omega_e F_{ds}\right) \quad \cdots\cdots\cdots (2.40)$$

$$V_{ds} = R_s i_{ds} + \frac{1}{\omega_b}\left(\frac{d}{dt}F_{ds} - \omega_e F_{qs}\right) \quad \cdots\cdots\cdots (2.41)$$

$$V_{qr} = R_r i_{qr} + \frac{1}{\omega_b}\left(\frac{d}{dt}F_{qr} + (\omega_e - \omega_r)F_{dr}\right) \quad \cdots\cdots\cdots (2.42)$$

$$V_{dr} = R_r i_{dr} + \frac{1}{\omega_b}\left(\frac{d}{dt}F_{dr} - (\omega_e - \omega_r)F_{qr}\right) \quad \cdots\cdots\cdots (2.43)$$

Multiplying by ω_b on both sides

$$F_{qs} = X_{ls} i_{qs} + X_m\left(i_{qs} + i_{qr}\right) \quad \cdots\cdots\cdots (2.44)$$

$$F_{qr} = X_{lr} i_{qr} + X_m\left(i_{qs} + i_{qr}\right) \quad \cdots\cdots\cdots (2.45)$$

$$F_{qm} = X_m\left(i_{qs} + i_{qr}\right) \quad \cdots\cdots\cdots (2.46)$$

$$F_{ds} = X_{ls} i_{ds} + X_m(i_{ds} + i_{dr}) \quad \cdots\cdots\cdots (2.47)$$

$$F_{dr} = X_{lr} i_{dr} + X_m(i_{ds} + i_{dr}) \quad \cdots\cdots\cdots (2.48)$$

$$F_{dm} = X_m(i_{ds} + i_{dr}) \quad \cdots\cdots\cdots (2.49)$$

Where, $X_{ls} = \omega_b L_{ls}$, $X_{lr} = \omega_b L_{lr}$, $X_m = \omega_b L_m$

Thus we have,

$$i_{qs} = \frac{F_{qs} - F_{qm}}{X_{ls}} \quad \cdots\cdots\cdots (2.50)$$

$$i_{qr} = \frac{F_{qr} - F_{qm}}{X_{lr}} \quad \cdots\cdots\cdots (2.51)$$

$$i_{ds} = \frac{F_{ds} - F_{dm}}{X_{ls}} \quad \cdots\cdots\cdots (2.52)$$

$$i_{dr} = \frac{F_{dr} - F_{dm}}{X_{lr}} \quad \cdots\cdots\cdots (2.53)$$

Substituting we have,

$$F_{qm} = X_m \left(\frac{F_{qs}-F_{qm}}{X_{ls}} + \frac{F_{qr}-F_{qm}}{X_{lr}}\right) \qquad \cdots\cdots\cdots (2.54)$$

$$F_{qm} = \frac{X_{m1}}{X_{ls}} F_{qs} + \frac{X_{m1}}{X_{lr}} F_{qr} \qquad \cdots\cdots\cdots (2.55)$$

Similarly,

$$F_{dm} = \frac{X_{m1}}{X_{ls}} F_{ds} + \frac{X_{m1}}{X_{lr}} F_{dr} \qquad \cdots\cdots\cdots (2.56)$$

Where,

$$X_{m1} = \frac{1}{\frac{1}{X_m}+\frac{1}{X_{ls}}+\frac{1}{X_{lr}}} \qquad \cdots\cdots\cdots (2.57)$$

Substituting we have,

$$V_{qs} = R_s \left(\frac{F_{qs}-F_{qm}}{X_{ls}}\right) + \frac{1}{\omega_b}\left(\frac{d}{dt}F_{qs} + \omega_e F_{ds}\right) \qquad \cdots\cdots\cdots (2.58)$$

$$V_{ds} = R_s \left(\frac{F_{ds}-F_{dm}}{X_{ls}}\right) + \frac{1}{\omega_b}\left(\frac{d}{dt}F_{ds} - \omega_e F_{qs}\right) \qquad \cdots\cdots\cdots (2.59)$$

$$V_{qr} = R_r \left(\frac{F_{qr}-F_{qm}}{X_{lr}}\right) + \frac{1}{\omega_b}\left(\frac{d}{dt}F_{qr} + (\omega_e - \omega_r) F_{dr}\right) \qquad \cdots\cdots\cdots (2.60)$$

$$V_{dr} = R_r \left(\frac{F_{dr}-F_{dm}}{X_{lr}}\right) + \frac{1}{\omega_b}\left(\frac{d}{dt}F_{dr} - (\omega_e - \omega_r) F_{qr}\right) \qquad \cdots\cdots\cdots (2.61)$$

This can be written in state space form as

$$\frac{d}{dt}F_{qs} = \omega_b \left[V_{qs} - \frac{\omega_e}{\omega_b}F_{ds} - R_s\left(\frac{F_{qs}-F_{qm}}{X_{ls}}\right)\right] \qquad \cdots\cdots\cdots (2.62)$$

$$\frac{d}{dt}F_{ds} = \omega_b \left[V_{ds} + \frac{\omega_e}{\omega_b}F_{qs} - R_s\left(\frac{F_{ds}-F_{dm}}{X_{ls}}\right)\right] \qquad \cdots\cdots\cdots (2.63)$$

$$\frac{d}{dt}F_{qr} = -\omega_b \left[\frac{(\omega_e-\omega_r)}{\omega_b}F_{dr} + R_r\left(\frac{F_{qr}-F_{qm}}{X_{lr}}\right)\right] \qquad \cdots\cdots\cdots (2.64)$$

$$\frac{d}{dt}F_{dr} = -\omega_b \left[-\frac{(\omega_e-\omega_r)}{\omega_b}F_{qr} + R_r\left(\frac{F_{dr}-F_{dm}}{X_{lr}}\right)\right] \qquad \cdots\cdots\cdots (2.65)$$

The Torque equation is

$$T_e = \frac{3}{2}\left(\frac{P}{2}\right)\frac{1}{\omega_b}\left(F_{ds}i_{qs} - F_{qs}i_{ds}\right) \qquad \cdots\cdots\cdots (2.66)$$

The rotor speed can be obtained from

$$\omega_r = \int_0^t \frac{P}{2J}(T_e - T_L)d\tau \qquad \cdots\cdots\cdots (2.67)$$

2.3 Direct Torque Control

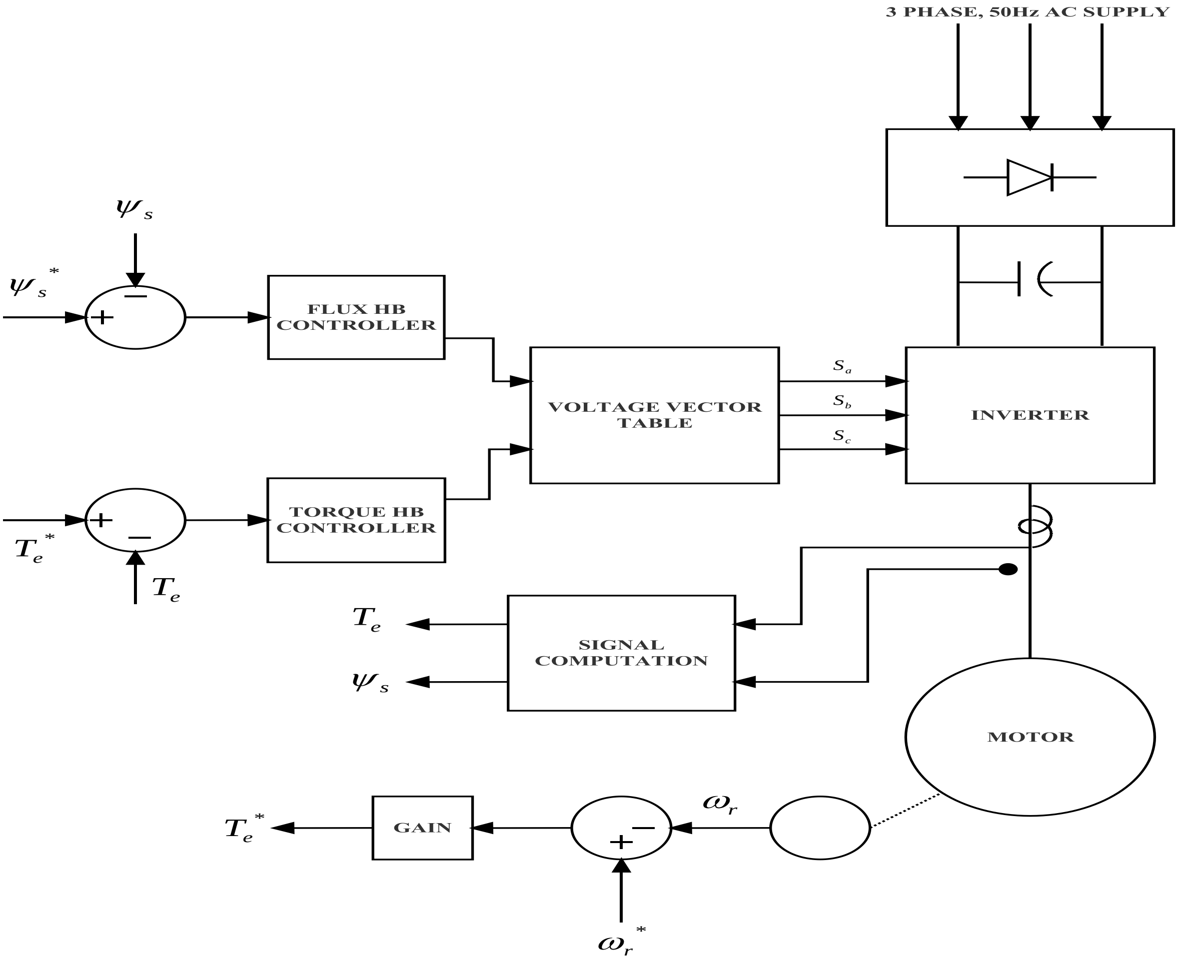

Figure 1.4: Block Diagram of Direct Torque Control Scheme

In this method the stator voltages and currents along with the rotor speed are measured. The stator voltage and current is used to determine the d-axis and q-axis flux linkages. These flux linkages are used to determine the net stator flux linkage. Using the data obtained from the flux linkages, the angle between rotor and stator flux linkages are obtained. Now with the help of the stator currents and flux linkages, the net electromagnetic torque is calculated. The actual flux linkage calculated is compared with the reference value to generate the flux error. The rotor speed is compared with the reference speed and the error is passed through a controller to generate the reference torque. This reference torque is compared with the actual torque calculated to generate the torque error. The flux and torque errors are passed through hysteresis controllers to give rise to the torque and flux command signals. Also the angle between the rotor and stator flux obtained earlier is used to determine the sector in which the stator flux linkage vector is present with respect to the rotor flux linkage vector. Thus the torque and flux command signals along with the sector data is fed to the processor where the optimum switching vector is determined with the help of a look up table. The switching vector is then used to trigger the required pulse signal to the switches in the VSI. This in turn controls the torque and hence speed of the motor according to the required conditions.

2.3.1 Concept behind Direct Torque Control

In stationary frame of reference

$$T_e = k\left(\frac{P}{2}\right)\left(\Psi_{ds} i_{qs} - \Psi_{qs} i_{ds}\right) \quad \cdots\cdots\cdots (2.68)$$

Now,

$$\Psi_{ds} = L_s i_{ds} + L_m i_{dr}$$

But,

$$i_{dr} = \frac{\Psi_{dr} - L_m i_{ds}}{L_r}$$

So,

$$\Psi_{ds} = L_s i_{ds} + \frac{L_m}{L_r}\Psi_{dr} - \frac{{L_m}^2}{L_r} i_{ds}$$

$$\Rightarrow \Psi_{ds} = \left(L_s - \frac{{L_m}^2}{L_r}\right) i_{ds} + \frac{L_m}{L_r}\Psi_{dr}$$

$$\Rightarrow \Psi_{ds} = L_s\left(1 - \frac{{L_m}^2}{L_s L_r}\right) i_{ds} + \frac{L_m}{L_r}\Psi_{dr}$$

$$\Rightarrow \Psi_{ds} = \sigma L_s i_{ds} + \frac{L_m}{L_r}\Psi_{dr} \quad \cdots\cdots\cdots (2.69)$$

Where $\sigma = 1 - \frac{{L_m}^2}{L_s L_r}$ is the leakage factor

So,

$$i_{ds} = \frac{1}{\sigma L_s}\left(\Psi_{ds} - \frac{L_m}{L_r}\Psi_{dr}\right) \quad \cdots\cdots\cdots (2.70)$$

Similarly,

$$i_{qs} = \frac{1}{\sigma L_s}\left(\Psi_{qs} - \frac{L_m}{L_r}\Psi_{qr}\right) \quad \cdots\cdots\cdots (2.71)$$

Substituting in the torque equation

$$T_e = k\left(\frac{P}{2}\right)\left(\frac{\Psi_{ds}}{\sigma L_s}\left(\Psi_{qs} - \frac{L_m}{L_r}\Psi_{qr}\right) - \frac{\Psi_{qs}}{\sigma L_s}\left(\Psi_{ds} - \frac{L_m}{L_r}\Psi_{dr}\right)\right)$$

$$\Rightarrow \; T_e = k\left(\frac{P}{2}\right)\frac{L_m}{\sigma L_s L_r}\left(\Psi_{qs}\Psi_{dr} - \Psi_{ds}\Psi_{qr}\right) \qquad \cdots\cdots\cdots (2.72)$$

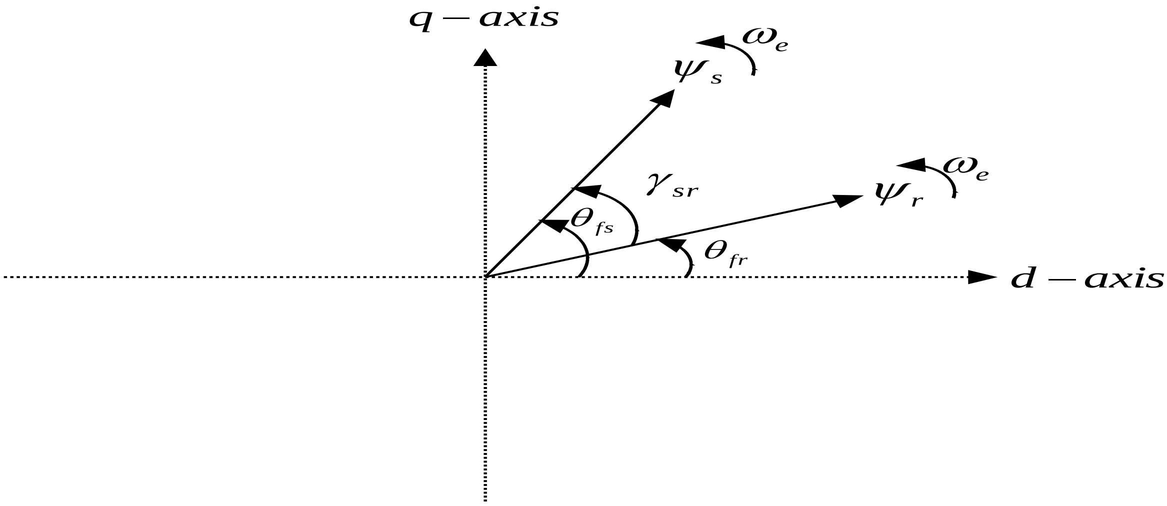

Figure 1.5: Stator and Rotor Flux linkage vectors

Let us consider stationary frame of reference. $\overrightarrow{\Psi_r}$ and $\overrightarrow{\Psi_s}$ are rotor and ststor flux vector rotating at synchronous speed but stationary with respect to each other.

Let γ_{sr} be the angle by which $\overrightarrow{\Psi_s}$ leads $\overrightarrow{\Psi_r}$.

Let at any instant, the angle between $\overrightarrow{\Psi_s}$ and d-axis be θ_{fs} and the angle between $\overrightarrow{\Psi_r}$ and d-axis be θ_{fr}

So,

$\Psi_{ds} = \left|\overrightarrow{\Psi_s}\right| \cos\theta_{fs}$

$\Psi_{dr} = \left|\overrightarrow{\Psi_r}\right| \cos\theta_{fr}$

$\Psi_{qs} = \left|\overrightarrow{\Psi_s}\right| \sin\theta_{fs}$

$\Psi_{qr} = \left|\overrightarrow{\Psi_r}\right| \sin\theta_{fr}$

Substituting in torque equation,

$$T_e = k\left(\frac{P}{2}\right)\frac{L_m}{\sigma L_s L_r}\left(|\overrightarrow{\Psi_s}||\overrightarrow{\Psi_r}|\sin\theta_{fs}\cos\theta_{fr} - |\overrightarrow{\Psi_s}||\overrightarrow{\Psi_r}|\cos\theta_{fs}\sin\theta_{fr}\right)$$

⇨ $T_e = k\left(\frac{P}{2}\right)\frac{L_m}{\sigma L_s L_r}\left(|\overrightarrow{\Psi_s}||\overrightarrow{\Psi_r}|\sin(\theta_{fs} - \theta_{fr})\right)$

⇨ $T_e = K|\overrightarrow{\Psi_s}||\overrightarrow{\Psi_r}|\sin(\gamma_{sr})$ ……… (2.73)

Thus the torque depends on

i) Magnitude of the two fluxes $\overrightarrow{\Psi_r}$ and $\overrightarrow{\Psi_s}$

ii) Sine of the angle between the two fluxes

Normally the flux is kept constant because either the machine will get saturated if flux is increased or it will be under-utilized if flux is reduced.

So, to control the torque the angle between the two fluxes is controlled using the space vectors.

Now,

$$\frac{d\overrightarrow{\Psi_s}}{dt} = \overrightarrow{V_s} - R_s\overrightarrow{\iota_s}$$

⇨ $\overrightarrow{\Psi_s} = \int_0^t (\overrightarrow{V_s} - R_s\overrightarrow{\iota_s})dt + \overrightarrow{\Psi_s}_{|t=0}$

⇨ $\overrightarrow{\Psi_s} = \int_0^t \overrightarrow{V_s}dt - \int_0^t R_s\overrightarrow{\iota_s}dt + \overrightarrow{\Psi_s}_{|t=0}$

Neglecting the resistance drop, $R_s = 0$

⇨ $\overrightarrow{\Psi_s} = \int_0^t \overrightarrow{V_s}dt + \overrightarrow{\Psi_s}_{|t=0}$

If we assume that the voltage vector remains constant for a small time Δt, we have

⇨ $\overrightarrow{\Psi_s} = \overrightarrow{V_s}\Delta t + \overrightarrow{\Psi_s}_{|t=0}$ ……… (2.74)

Hence by using various voltage vectors we can vary $\overrightarrow{\Psi_s}$. Thus the angle between $\overrightarrow{\Psi_r}$ and $\overrightarrow{\Psi_s}$ can be varied and used to control the torque.

2.4 Simulation Equations and Model

Flux Linkage Equations

$$\Psi_{ds} = \int_0^t \left(V_{ds} - R_s i_{ds} + \omega_e \Psi_{qs}\right) d\tau \qquad \cdots\cdots\cdots (2.75)$$

$$\Psi_{qs} = \int_0^t \left(V_{qs} - R_s i_{qs} - \omega_e \Psi_{ds}\right) d\tau \qquad \cdots\cdots\cdots (2.76)$$

So, in state space form

$$\begin{bmatrix} \dot{\Psi}_{ds} \\ \dot{\Psi}_{qs} \end{bmatrix} = \begin{bmatrix} V_{ds} \\ V_{qs} \end{bmatrix} - R_s \begin{bmatrix} i_{ds} \\ i_{qs} \end{bmatrix} - \omega_e \begin{bmatrix} 0 & -1 \\ 1 & 0 \end{bmatrix} \begin{bmatrix} \Psi_{ds} \\ \Psi_{qs} \end{bmatrix} \qquad \cdots\cdots\cdots (2.77)$$

Similarly,

$$\Psi_{dr} = \int_0^t \left(-R_r i_{dr} + (\omega_e - \omega_r)\Psi_{qr}\right) d\tau \qquad \cdots\cdots\cdots (2.78)$$

$$\Psi_{qr} = \int_0^t \left(-R_r i_{qr} - (\omega_e - \omega_r)\Psi_{dr}\right) d\tau \qquad \cdots\cdots\cdots (2.79)$$

So,

$$\begin{bmatrix} \dot{\Psi}_{dr} \\ \dot{\Psi}_{qr} \end{bmatrix} = -R_s \begin{bmatrix} i_{dr} \\ i_{qr} \end{bmatrix} - (\omega_e - \omega_r) \begin{bmatrix} 0 & -1 \\ 1 & 0 \end{bmatrix} \begin{bmatrix} \Psi_{dr} \\ \Psi_{qr} \end{bmatrix} \qquad \cdots\cdots\cdots (2.80)$$

Current Equations

$$i_{ds} = \frac{\Psi_{ds} - L_m i_{dr}}{L_{ls} + L_m} \qquad \cdots\cdots\cdots (2.81)$$

$$i_{qs} = \frac{\Psi_{qs} - L_m i_{qr}}{L_{ls} + L_m} \qquad \cdots\cdots\cdots (2.82)$$

$$i_{dr} = \frac{\Psi_{dr} - L_m i_{ds}}{L_{lr} + L_m} \qquad \cdots\cdots\cdots (2.83)$$

$$i_{qr} = \frac{\Psi_{qr} - L_m i_{qs}}{L_{lr} + L_m} \qquad \cdots\cdots\cdots (2.84)$$

Torque Equations

$$T_e = \frac{3}{2}\left(\frac{P}{2}\right)\left(\Psi_{ds} i_{qs} - \Psi_{qs} i_{ds}\right) \qquad \cdots\cdots\cdots (2.85)$$

$$T_e = 0.75P \left[\begin{bmatrix} 0 & -1 \\ 1 & 0 \end{bmatrix} \begin{bmatrix} \Psi_{ds} \\ \Psi_{qs} \end{bmatrix}\right] \cdot \begin{bmatrix} i_{ds} \\ i_{qs} \end{bmatrix} \qquad \cdots\cdots\cdots (2.86)$$

$$\omega_r = \int_0^t \frac{P}{2J}\left(T_e - T_L - B_m \omega_r\right) d\tau \qquad \cdots\cdots\cdots (2.87)$$

Where, B_m is the damping coefficient

The overall Simulink model is given in figure 1.6

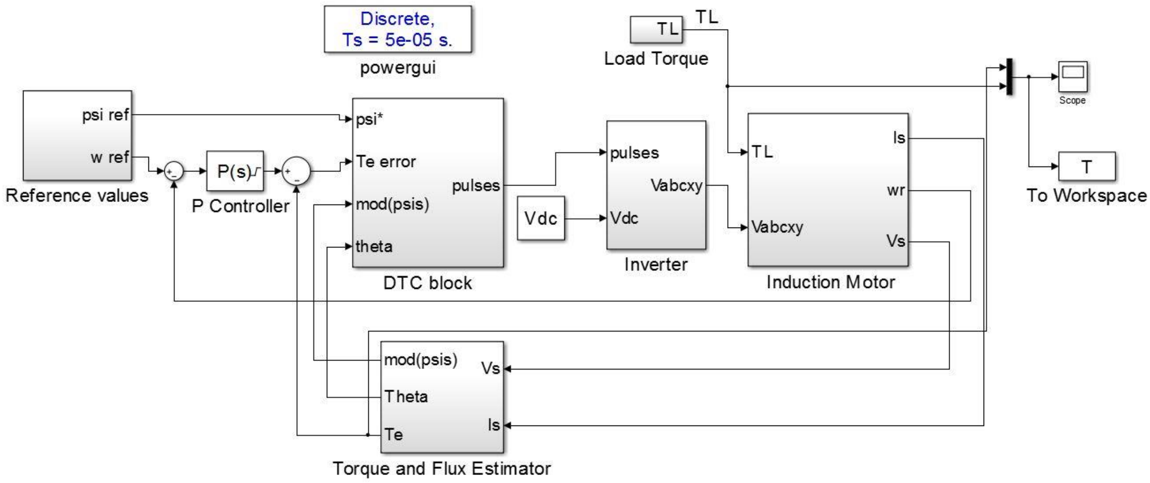

Figure 1.6: Simulink model of the entire DTC process

The Simulink model of the three phase Induction motor is given in figure 1.7

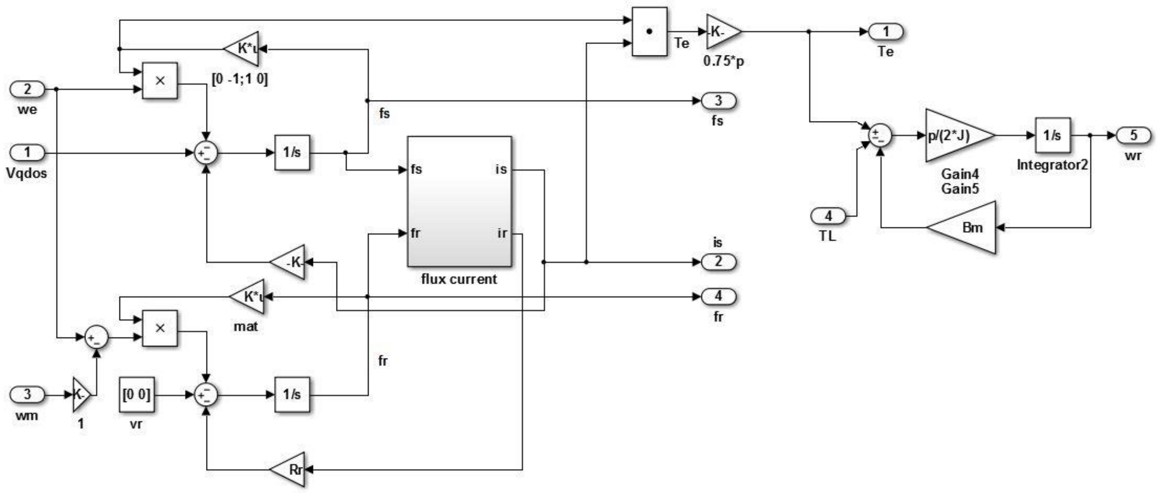

Figure 1.7: Simulink Model of Induction motor modelling

2.5 Summary

In this chapter the process of axes transformation from three phase variables to two mutually orthogonal axes was introduced. Using this transformation, the phase equivalent model of an induction motor was obtained and the equations for modelling the induction motor were derived. The concept of DTC was also studied and it was observed that the torque can be controlled by varying the angle between the stator and rotor flux linkage vectors.

Chapter 3

DTC in Three Phase Induction Motor

The primary requirement of a three phase induction motor drive is a three phase ac supply whose magnitude, phase and frequency can be controlled. Such a supply cannot be obtained directly from the grid. Hence a three phase power electronic converter is used to convert a dc supply into a controlled three phase ac supply. These converters are of two types. One is where the output voltage is independently controlled. Such are called Voltage Source Converters and the other is where current is independently controlled. Such are called Current Source Inverters. The voltage source inverters (VSI) are generally more preferred because they behave as voltage sources which are required for several applications.

3.1 Three Phase Voltage Source Inverter

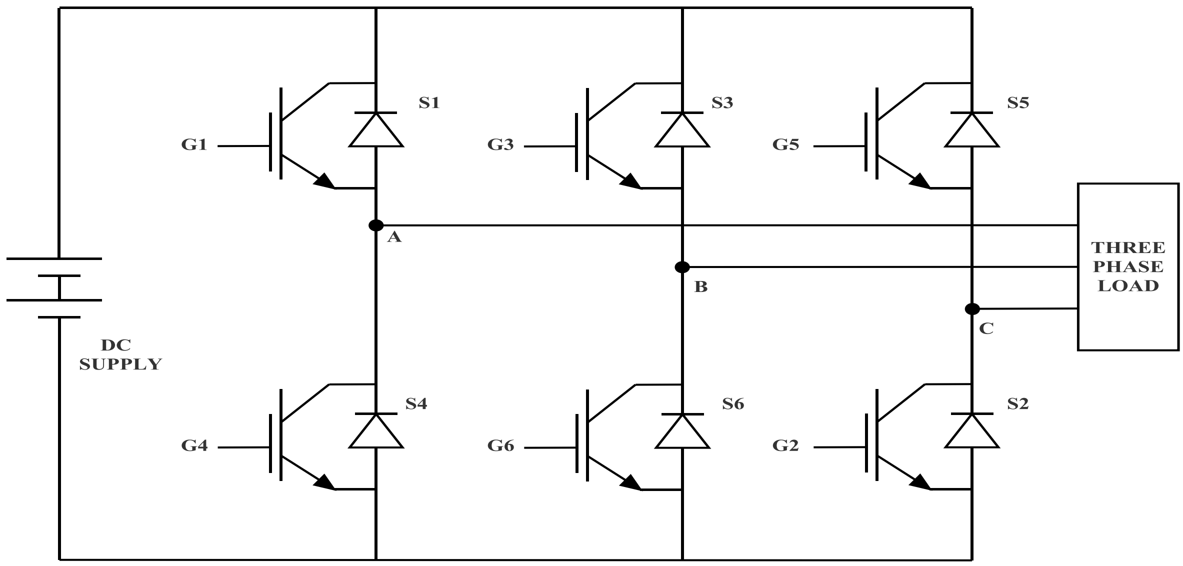

Figure 3.1: Circuit Diagram of three phase VSI

To obtain three phase supply for the induction motor, a three phase VSI is used to invert the input dc voltage into three phase supply. The three phase VSI uses six power switches which can be either MOSFET, IGBT or any other power electronic switches. The use of thyristors is not recommended due to its complex commutation circuit. In this simulation IGBTs are used. The inversion process can occur in two different modes. One is the 120° mode and the other one is 180° mode. In the 120° mode, each switch conducts for a period of 120° and then remains switched off for the rest of the cycle. In the 180° mode, each switch remains on for 180°, i.e. for one half cycle and switched off for the other half cycle. The advantage of the 180° mode of conduction is that in this mode all the three legs of the VSI are conducting at any point of time. So the potential of all three legs are well defined irrespective of the load. However, in the 120° mode, only two legs conduct at a time and neither of the switches in the third leg conduct. So the potential of this third leg is not well defined and is dependent on the type of load attached. On the other hand in 180° mode, there is a chance of direct short circuit if a commutation interval is not provided while switching from one switch to another switch of the same leg. This problem is avoided in 120° mode of conduction. In this project, we have used 180° mode of conduction for the sake of simplicity.

3.1.1 180° mode of conduction:

As we can see from the figure 3.1, there are six switches in the VSI, each one triggered separately from a firing circuit. In the 180° mode of conduction, each of the six switches conduct for a period of 180° or one half cycle in a complete cycle. As one cycle consists of 360° and there are six switches, there are 6 steps in the three phase VSI with each step being of 60° duration. The duration of switching between any switches on the same leg is 180° and two neighboring switches on the same arm is 120°. According to the index, the switches are triggered at a difference of 60°. The switching pulse for the six switches is shown in figure 3.2.

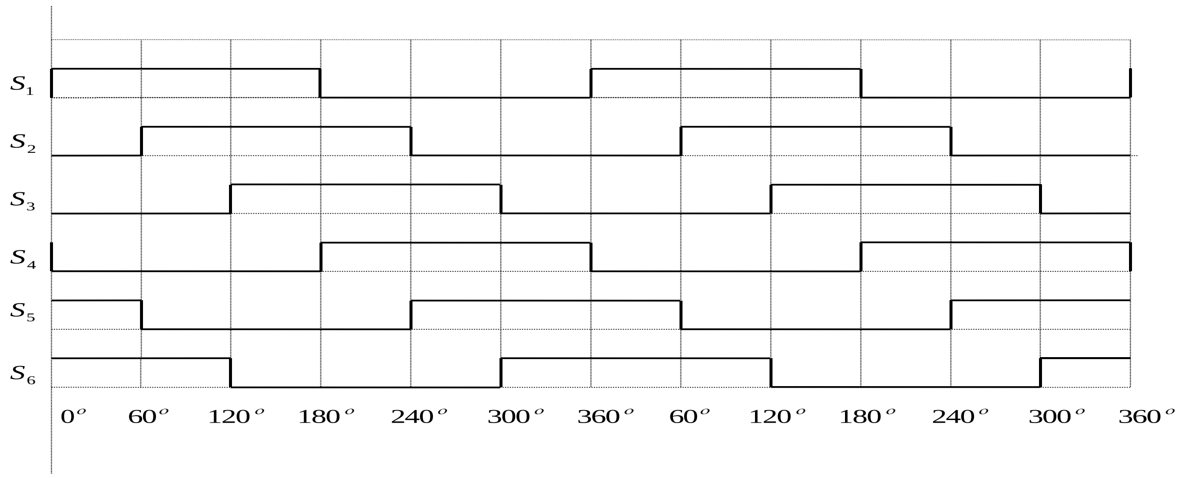

Figure 3.2: Switching Pulse waveform in a three phase VSI

As we can see for the first duration i.e. from 0° to 60°, switches S_5, S_6 and S_1 conduct. Thus the path of the current is Battery→S_1 and S_5→S_6→Battery. Thus the upper arm of phase a & c conduct whereas the lower arm of phase b conduct. Therefore, the phase voltages are positive in phase a & c, while it is negative in phase b. The conducting switches for each step of the cycle are as follows.

0° to 60° : S_5, S_6, S_1

60° to 120° : S_6, S_1, S_2

120° to 180° : S_1, S_2, S_3

180° to 240° : S_2, S_3, S_4

240° to 300° : S_3, S_4, S_5

300° to 360° : S_4, S_5, S_6

Assuming, equal load impedence on each of the phases, the magnitude of phase voltage is $\frac{V}{3}$ in the phases where two switches are on in the same arm and the magnitude is $\frac{2V}{3}$ in the remaining phase. This can be easily verified using voltage division rule. The sign depends on whether the switch is on upper arm or lower. For the upper arm, the sign is positive, whereas, for the lower arm, the sign is negative. The waveforms for the phase voltage are shown in figure 3.3.

Figure 3.3: Phase Voltage waveform in a three phase VSI

3.2 State Vectors in a three phase VSI

From the figure 3.1 we can see that at a time only one switch of each leg can conduct. So for each leg we can say that only two conditions exist. The first one is that the switch in the upper arm will conduct (state 1) and the second one is that the switch in the lower arm will conduct (state 0). Thus for the VSI having 3 legs and with each leg having two states, the total possible states available in a three phase VSI is $2^3 = 8$. Out of these eight possible states, the states 000 and 111 are insignificant because they represent open path. The phase voltages can be obtained from the following matrix by substituting the state of the leg in each phase.

$$\begin{bmatrix} V_{as} \\ V_{bs} \\ V_{cs} \end{bmatrix} = \frac{V_{dc}}{3} \begin{bmatrix} 2 & -1 & -1 \\ -1 & 2 & -1 \\ -1 & -1 & 2 \end{bmatrix} \begin{bmatrix} S_a \\ S_b \\ S_c \end{bmatrix} \qquad \cdots\cdots\cdots (3.1)$$

Here, S_a, S_b, S_c represent the state of each leg at the point of time being considered.

For example, let us consider the step duration of 0° to 60°. From figure 3.1 we can see that during this duration upper arms of phase a & c are on whereas lower arm of phase b is on. So, we can easily say that $S_a = 1$, $S_b = 0$, and $S_c = 1$.

Putting these values in the matrix we obtain

$$\begin{bmatrix} V_{as} \\ V_{bs} \\ V_{cs} \end{bmatrix} = \frac{V_{dc}}{3} \begin{bmatrix} 2 & -1 & -1 \\ -1 & 2 & -1 \\ -1 & -1 & 2 \end{bmatrix} \begin{bmatrix} 1 \\ 0 \\ 1 \end{bmatrix}$$

Thus, we have the phase voltages as

$$\begin{bmatrix} V_{as} \\ V_{bs} \\ V_{cs} \end{bmatrix} = \frac{V_{dc}}{3} \begin{bmatrix} 1 \\ -2 \\ 1 \end{bmatrix}$$

These exactly matches with the voltages that we can find from figure 3.3.

Now, from equation 2.6 and 2.7, in the stationary frame of reference,

$$\begin{bmatrix} V_{qs}{}^{s} \\ V_{ds}{}^{s} \end{bmatrix} = \frac{2}{3} \begin{bmatrix} 1 & \cos(-120°) & \cos(+120°) \\ 0 & \sin(-120°) & \sin(+120°) \end{bmatrix} \begin{bmatrix} V_{as} \\ V_{bs} \\ V_{cs} \end{bmatrix}$$

$$\vec{V_s} = \frac{2}{3}\left[V_{as} + V_{bs}e^{i2\pi/3} + V_{cs}e^{-i2\pi/3}\right]$$

From the above complex form of space vector we can say that each space vector has a magnitude and a phase angle. The list of all eight space vectors along with their magnitudes and phase angles are given in table 3.1

Table 3.1: List of switching state vectors in a three phase VSI

$\overline{V_s}$	**Van**	**Vbn**	**Vcn**	**Switch Status (abc)**	**Magnitude**	**Angle(°)**
$\overline{V0}$	0	0	0	0 0 0	0	-
$\overline{V1}$	$\frac{2}{3}Vo$	$\frac{-1}{3}Vo$	$\frac{-1}{3}Vo$	1 0 0	$2\,Vo\,/3$	0
$\overline{V2}$	$\frac{1}{3}Vo$	$\frac{1}{3}Vo$	$\frac{-2}{3}Vo$	1 1 0	$2\,Vo\,/3$	60
$\overline{V3}$	$\frac{-1}{3}Vo$	$\frac{2}{3}Vo$	$\frac{-1}{3}Vo$	0 1 0	$2\,Vo\,/3$	120
$\overline{V4}$	$\frac{-2}{3}Vo$	$\frac{1}{3}Vo$	$\frac{1}{3}Vo$	0 1 1	$2\,Vo\,/3$	180
$\overline{V5}$	$\frac{-1}{3}Vo$	$\frac{-1}{3}Vo$	$\frac{2}{3}Vo$	0 0 1	$2\,Vo\,/3$	240
$\overline{V6}$	$\frac{1}{3}Vo$	$\frac{-2}{3}Vo$	$\frac{1}{3}Vo$	1 0 1	$2\,Vo\,/3$	300
$\overline{V7}$	0	0	0	1 1 1	0	-

Example:

Let us consider the case of V2

Here, $(S_a = 1, S_b = 1, S_c = 0)$

So, $V_{an} = \frac{1}{3}Vo, V_{bn} = \frac{1}{3}Vo, V_{cn} = \frac{-2}{3}Vo$

Putting this values in the complex equation we have

$$\overrightarrow{V2} = \frac{2Vo}{3}\left[\frac{1}{3} + \frac{1}{3}e^{i2\pi/3} + \frac{-2}{3}e^{-i2\pi/3}\right]$$

$$\overrightarrow{V2} = 1 * \frac{2Vo}{3}\angle 60°$$

3.3 Look-up Table for Three phase DTC

The state vector diagram for the switching vectors in table 3.1 is shown in figure 3.4. This diagram gives us a complete idea about the magnitude and space orientation of the space vectors. This is useful to choose the optimum switching vector as per our requirement.

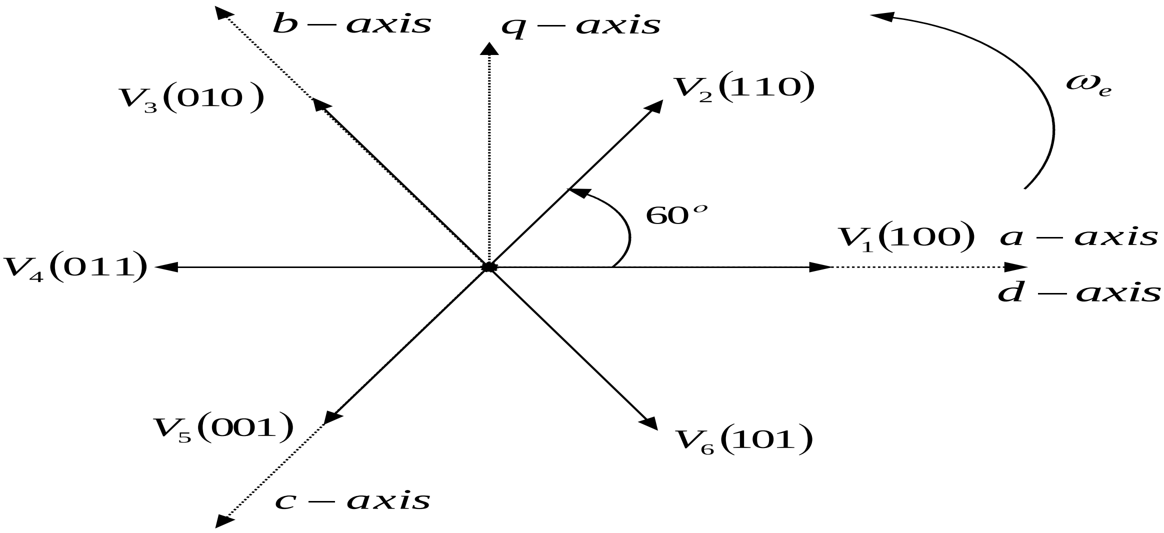

Figure 3.4: State vector diagram in a three phase VSI

The entire space is now divided into six sectors each spanning 60°. Figure 3.5 shows the sector distribution of the space. Here S_1 to S_6 represent the six sectors.

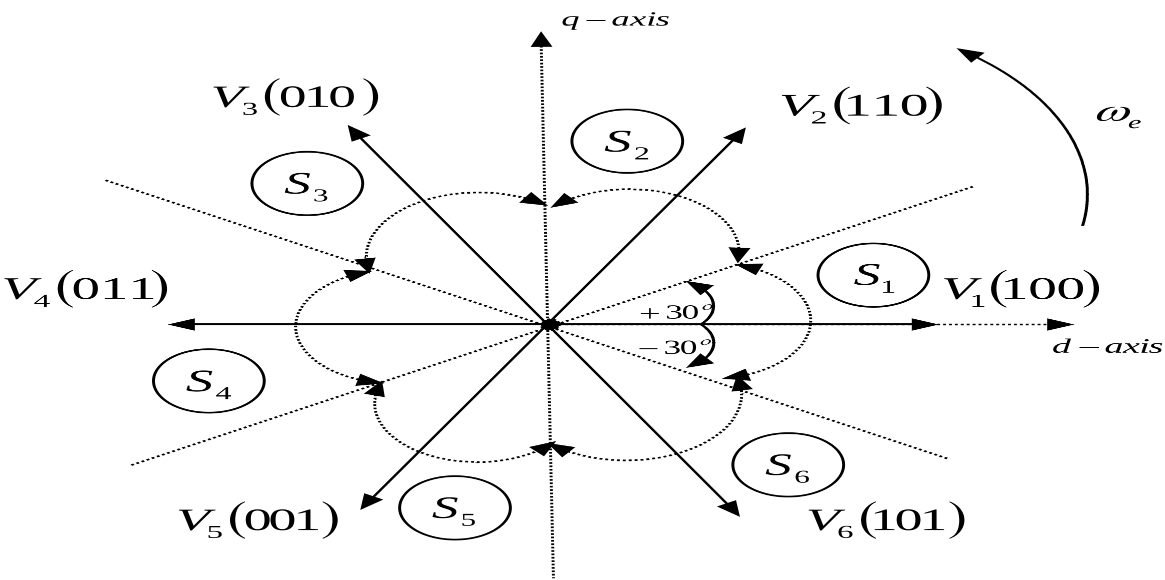

Figure 3.5: Sector distribution in the state vector diagram in a three phase VSI

Let rotor flux be along d-axis and stator flux leads the rotor flux by some angle towards the q-axis. Let us assume that the stator flux vector is in sector 1. As we can observe, voltage vectors V1, V2, V6 can increase the magnitude of the flux while voltage vectors V4, V3, V5 can decrease the magnitude of flux. Similarly, V2, V3, V4 can increase the torque where as V1, V6, V5 can decrease it.

Thus,

V1, V2, V6 – increase flux and V4, V3, V5 – decrease flux

V2, V3, V4 – increase torque and V1, V6, V5 – decrease torque

In DTC, H_Ψ, H_{Te} and sector are given as input to the look up table to decide appropriate voltage vector.

Now,

H_Ψ is the error obtained when the actual flux linkage vector is subtracted from the reference flux linkage vector. Thus when the actual flux linkage vector is less than the reference vector, the error becomes positive. This positive value is then passed through the hysteresis controller. If the positive error so obtained is greater than the upper tolerance value, the output from the hysteresis controller is 1. This instructs the processor to increase the flux linkage. Similarly, when the actual flux linkage vector is higher than the reference vector, the error becomes negative. If the negative error so obtained is more negative than the lower tolerance value, the output from the hysteresis controller is -1. This instructs the processor to decrease the flux linkage.

Thus,

$H_\Psi = 1 \rightarrow \Psi_s^* > \Psi_s$ (So flux linkage has to be increased)

$H_\Psi = -1 \rightarrow \Psi_s^* < \Psi_s$ (So flux linkage has to be decreased)

Similarly,

H_{Te} is the error obtained when the actual torque vector is subtracted from the reference torque vector. Thus when the actual torque vector is less than the reference vector, the error becomes positive. This positive value is then passed through the hysteresis controller. If the positive error so obtained is greater than the upper tolerance value, the output from the hysteresis controller is 1. This instructs the processor to increase the torque. Similarly, when the actual torque vector is higher than the reference vector, the error becomes negative. If the negative error so obtained is more negative than the lower tolerance value, the output from the hysteresis controller is -1. This instructs the processor to decrease the torque. However, if the torque error is negligible and is within the mid-band region, the output is zero. This instructs the processor not to do any change in the torque values.

Thus

H_{Te} = 1 → $T_e{}^* > T_e$ (Torque has to be increased)

H_{Te} = 0 → $T_e{}^* = T_e$ (No change)

H_{Te} = -1 → $T_e{}^* < T_e$ (Torque has to be decreased)

Using all these criteria we can determine the optimum switching vector for the following cases. Let us assume that for all cases the sector is 1.

Case1: To decrease both flux and torque, we should choose V_5

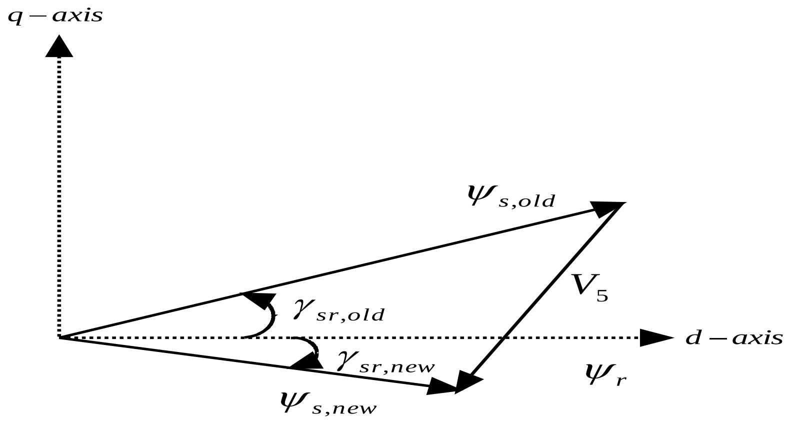

Figure 3.6: Effect of switching vector V_5

Case2: To decrease flux but increase torque, we should choose V_3

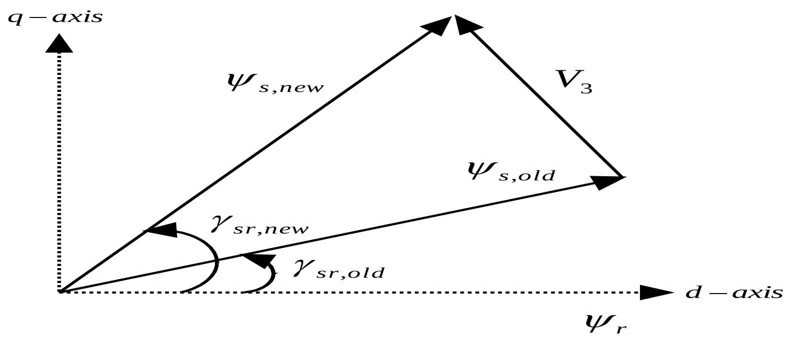

Figure 3.7: Effect of switching vector V_3

Case3: To increase flux but decrease torque, we should choose V_6

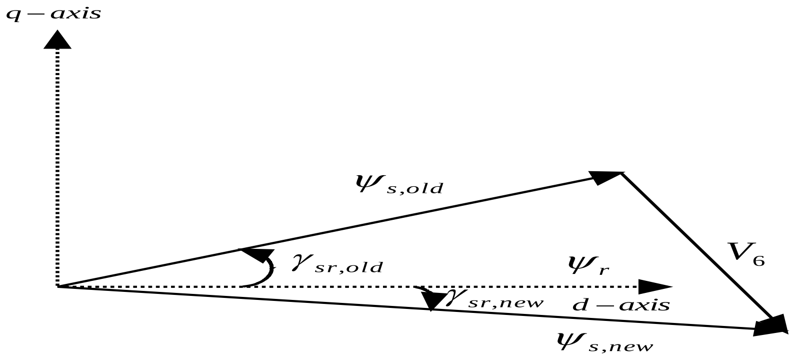

Figure 3.8: Effect of switching vector 6

Case4: To increase both flux and torque, we should choose V_2

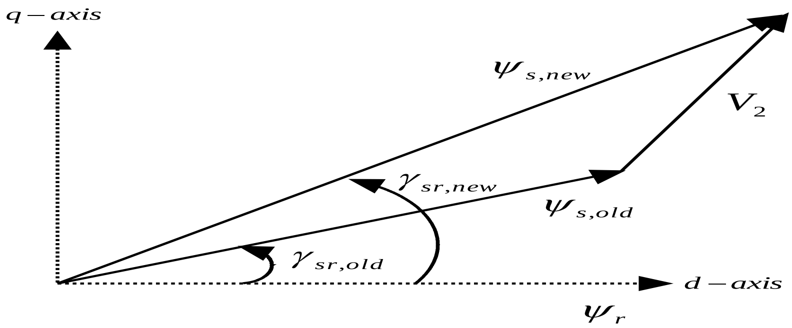

Figure 3.9: Effect of switching vector V_2

Similarly, we can find the optimum switching vector for other sectors too. The look up table for obtaining DTC in a three phase IM is given in table 3.2

Table 3.2: Look up table for DTC in a three phase induction motor

H_ψ	H_{Te}	Sector 1	Sector 2	Sector 3	Sector 4	Sector 5	Sector 6
-1	**-1**	5	6	1	2	3	4
	0	7	0	7	0	7	0
	1	3	4	5	6	1	2
1	**-1**	6	1	2	3	4	5
	0	0	7	0	7	0	7
	1	2	3	4	5	6	1

3.4 Simulink Model

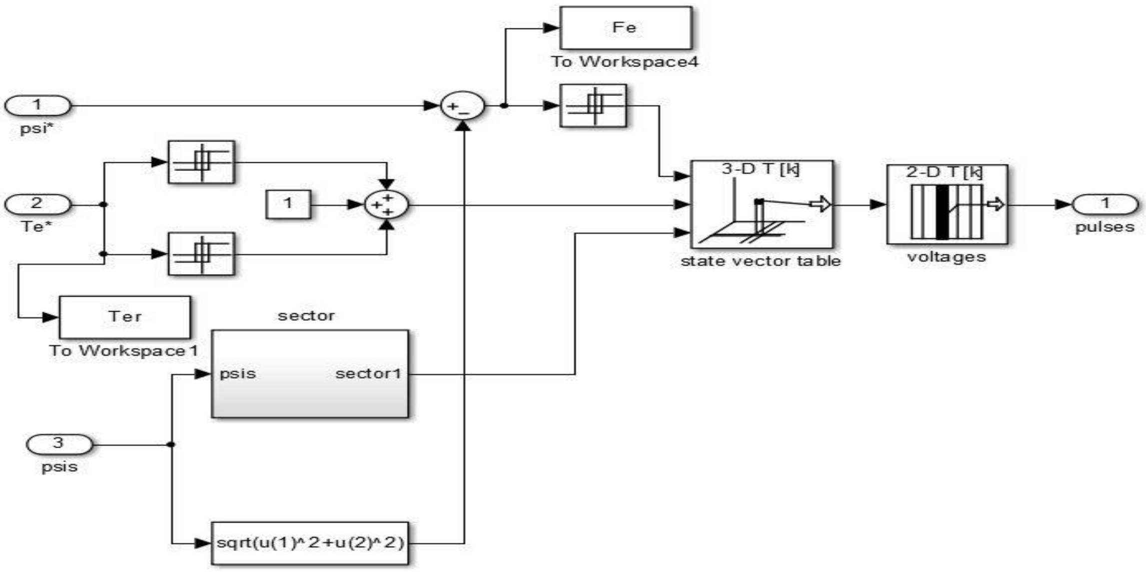

Figure 3.10: Simulink Model of the DTC block in a three phase induction motor

3.5 Summary

In this chapter we studied about the switching patterns in a three phase VSI and obtained the eight possible switching states. Out of these eight switching states only six are active while the rest two are null vectors. Using the complex form of the vector space equation the magnitude and phase of each vectors were used to create the state vector diagram. The effect of each switching vector in changing the torque and flux of the system was studied. Based on these observations, a look up table was designed which will be used to choose the optimum switching state based on the torque error, flux error and the sector information.

Chapter 4

DTC in Five Phase Induction Motor

The five phase induction motor possess a lot of advantages as compared to the three phase machine as mentioned in chapter 1. However, for the machine to run, a five phase controllable ac supply is required. Hence similar to the three phase VSI, here a five phase VSI is used which converts the dc supply into balanced five phase supply. The five phase VSI has five legs and ten switches compared to three legs and six switches for a three phase machine. It is in fact, due to these extra features of the five phase VSI, DTC in a five phase induction motor drive is more efficient.

4.1 Axes Transformation

A five phase supply consists of five voltage vectors time displaced with each other by 72°. Let these vectors be a,b,c,ds & e. Here we have used 'ds' phase to differentiate it from d-axis. Just like in case of three phase voltage vectors, the five phase voltage vectors can be transformed into two mutually perpendicular voltage vectors along the d^s $axis$ and q^s axis in the stationary reference frame.

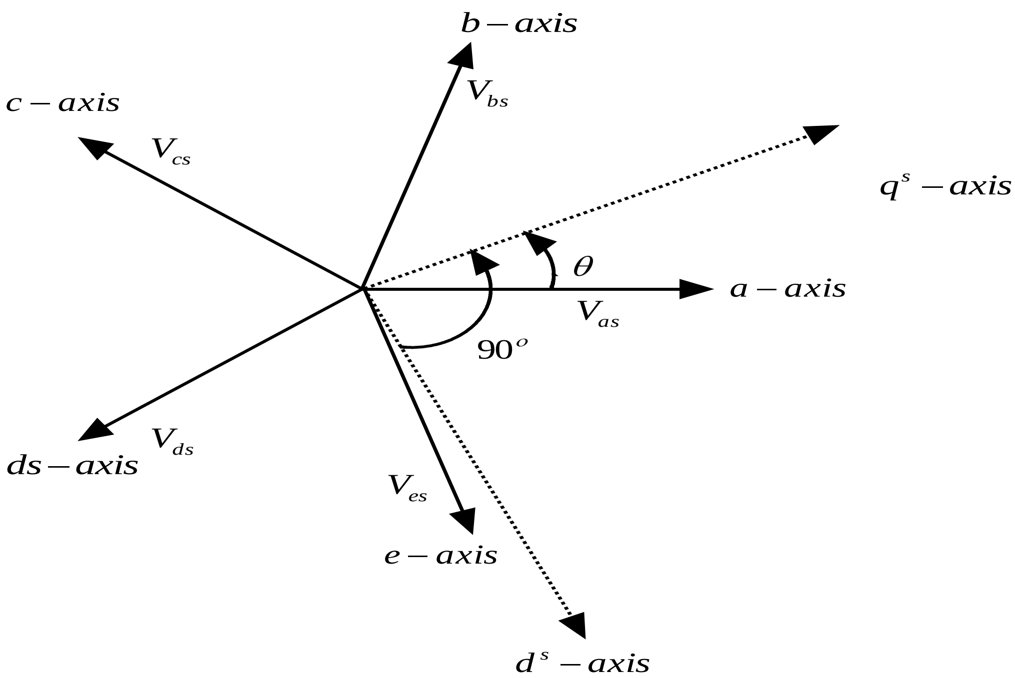

Figure 4.1: Transformation of a-b-c-ds-e axis to d^s-q^s axis

From the figure 4.1, we can resolve the phase voltages into V_d and V_q components present along $d^s\ axis$ and q^s axis respectively [16].

Now from the above figure

$$V_{an} = V_q \cos\theta + V_d \sin\theta \qquad \cdots\cdots\cdots (4.1)$$

$$V_{bn} = V_q \cos(\theta - 2\pi/5) + V_d \sin(\theta - 2\pi/5) \qquad \cdots\cdots\cdots (4.2)$$

$$V_{cn} = V_q \cos(\theta - 4\pi/5) + V_d \sin(\theta - 4\pi/5) \qquad \cdots\cdots\cdots (4.3)$$

$$V_{dn} = V_q \cos(\theta + 4\pi/5) + V_d \sin(\theta + 4\pi/5) \qquad \cdots\cdots\cdots (4.4)$$

$$V_{en} = V_q \cos(\theta + 2\pi/5) + V_d \sin(\theta + 2\pi/5) \qquad \cdots\cdots\cdots (4.5)$$

So,

$$\begin{bmatrix} V_{an} \\ V_{bn} \\ V_{cn} \\ V_{dn} \\ V_{en} \end{bmatrix} = \begin{bmatrix} \cos\theta & \sin\theta & 1 \\ \cos(\theta - 2\pi/5) & \sin(\theta - 2\pi/5) & 1 \\ \cos(\theta - 4\pi/5) & \sin(\theta - 4\pi/5) & 1 \\ \cos(\theta + 4\pi/5) & \sin(\theta + 4\pi/5) & 1 \\ \cos(\theta + 2\pi/5) & \sin(\theta + 2\pi/5) & 1 \end{bmatrix} \begin{bmatrix} V_q \\ V_d \\ V_0 \end{bmatrix} \qquad \cdots\cdots\cdots (4.6)$$

Taking inverse of the matrix, we have

$$\begin{bmatrix} V_q \\ V_d \\ V_0 \end{bmatrix} = \frac{2}{5} \begin{bmatrix} \cos\theta & \cos(\theta - 2\pi/5) & \cos(\theta - 4\pi/5) & \cos(\theta + 4\pi/5) & \cos(\theta + 2\pi/5) \\ \sin\theta & \sin(\theta - 2\pi/5) & \sin(\theta - 4\pi/5) & \sin(\theta + 4\pi/5) & \sin(\theta + 2\pi/5) \\ 1/2 & 1/2 & 1/2 & 1/2 & 1/2 \end{bmatrix} \begin{bmatrix} V_{an} \\ V_{bn} \\ V_{cn} \\ V_{dn} \\ V_{en} \end{bmatrix}$$

$$\cdots\cdots\cdots (4.7)$$

A zero sequence component doesn’t exist in a star connected multiphase machine without neutral connection for odd phase numbers.

$$\begin{bmatrix} V_q \\ V_d \end{bmatrix} = \frac{2}{5} \begin{bmatrix} \cos\theta & \cos(\theta - 2\pi/5) & \cos(\theta - 4\pi/5) & \cos(\theta + 4\pi/5) & \cos(\theta + 2\pi/5) \\ \sin\theta & \sin(\theta - 2\pi/5) & \sin(\theta - 4\pi/5) & \sin(\theta + 4\pi/5) & \sin(\theta + 2\pi/5) \end{bmatrix} \begin{bmatrix} V_{an} \\ V_{bn} \\ V_{cn} \\ V_{dn} \\ V_{en} \end{bmatrix}$$

$$\cdots\cdots\cdots (4.8)$$

Assuming $\theta = 0$, we can write in complex form as

$$\vec{V_s} = V_q - jV_d$$

⇨ $\vec{V_s} = V_{an}[1 - j0] + V_{bn}[\cos(-2\pi/5) - j\sin(-2\pi/5)] + V_{cn}[\cos(-4\pi/5) - j\sin(-4\pi/5)] + V_{dn}[\cos(4\pi/5) - j\sin(4\pi/5)] + V_{en}[\cos(2\pi/5) - j\sin(2\pi/5)]$

⇨ $\vec{V_s} = V_{an} + V_{bn}[\cos(2\pi/5) + j\sin(2\pi/5)] + V_{cn}[\cos(4\pi/5) + j\sin(4\pi/5)] + V_{dn}[\cos(-4\pi/5) + j\sin(-4\pi/5)] + V_{en}[\cos(-2\pi/5) + j\sin(-2\pi/5)]$

Because, $\sin(-\theta) = -\sin\theta$ and $\cos(-\theta) = \cos\theta$

$$\vec{V_s} = \frac{2}{5}\left[V_{an} + V_{bn}e^{i2\pi/5} + V_{cn}e^{i4\pi/5} + V_{dn}e^{-i4\pi/5} + V_{en}e^{-i2\pi/5}\right] \qquad \cdots\cdots\cdots (4.9)$$

4.2 Induction Motor Modelling

As the phase equivalent circuit of any induction machine is same, the modelling equations for voltage, flux and currents in a five phase induction machine is same as that of a three phase machine. Thus here also the equations used for simulation are:

Flux Linkage Equations

$$\Psi_{ds} = \int_0^t \left(V_{ds} - R_s i_{ds} + \omega_e \Psi_{qs}\right) d\tau \qquad \cdots\cdots\cdots (4.10)$$

$$\Psi_{qs} = \int_0^t \left(V_{qs} - R_s i_{qs} - \omega_e \Psi_{ds}\right) d\tau \qquad \cdots\cdots\cdots (4.11)$$

So, in state space form

$$\begin{bmatrix} \dot{\Psi}_{ds} \\ \dot{\Psi}_{qs} \end{bmatrix} = \begin{bmatrix} V_{ds} \\ V_{qs} \end{bmatrix} - R_s \begin{bmatrix} i_{ds} \\ i_{qs} \end{bmatrix} - \omega_e \begin{bmatrix} 0 & -1 \\ 1 & 0 \end{bmatrix} \begin{bmatrix} \Psi_{ds} \\ \Psi_{qs} \end{bmatrix} \qquad \cdots\cdots\cdots (4.12)$$

Similarly,

$$\Psi_{dr} = \int_0^t \left(-R_r i_{dr} + (\omega_e - \omega_r)\Psi_{qr}\right) d\tau \qquad \cdots\cdots\cdots (4.13)$$

$$\Psi_{qr} = \int_0^t \left(-R_r i_{qr} - (\omega_e - \omega_r)\Psi_{dr}\right) d\tau \qquad \cdots\cdots\cdots (4.14)$$

So,

$$\begin{bmatrix} \dot{\Psi}_{dr} \\ \dot{\Psi}_{qr} \end{bmatrix} = -R_s \begin{bmatrix} i_{dr} \\ i_{qr} \end{bmatrix} - (\omega_e - \omega_r) \begin{bmatrix} 0 & -1 \\ 1 & 0 \end{bmatrix} \begin{bmatrix} \Psi_{dr} \\ \Psi_{qr} \end{bmatrix} \qquad \cdots\cdots\cdots (4.15)$$

Current Equations

$$i_{ds} = \frac{\Psi_{ds} - L_m i_{dr}}{L_{ls} + L_m} \quad \cdots\cdots\cdots (4.16)$$

$$i_{qs} = \frac{\Psi_{qs} - L_m i_{qr}}{L_{ls} + L_m} \quad \cdots\cdots\cdots (4.17)$$

$$i_{dr} = \frac{\Psi_{dr} - L_m i_{ds}}{L_{lr} + L_m} \quad \cdots\cdots\cdots (4.18)$$

$$i_{qr} = \frac{\Psi_{qr} - L_m i_{qs}}{L_{lr} + L_m} \quad \cdots\cdots\cdots (4.19)$$

Torque Equations

However, the torque equations are different from those in three phase machine.

The torque equation in a five phase machine is

$$T_e = \frac{5}{2}\left(\frac{P}{2}\right)\left(\Psi_{ds} i_{qs} - \Psi_{qs} i_{ds}\right) \quad \cdots\cdots\cdots (4.20)$$

$$T_e = 1.25P \left[\begin{bmatrix} 0 & -1 \\ 1 & 0 \end{bmatrix} \begin{bmatrix} \Psi_{ds} \\ \Psi_{qs} \end{bmatrix}\right] \cdot \begin{bmatrix} i_{ds} \\ i_{qs} \end{bmatrix}$$

$$\omega_r = \int_0^t \frac{P}{2J} (T_e - T_L - B_m \omega_r) d\tau$$

Where, B_m is the damping coefficient

4.3 Five Phase VSI

Just like the case of a three phase VSI, the five phase VSI provides the required five phase supply to the IM from the dc supply. It consists of five legs with two power electronic switches in each leg. Thus there are a total of ten power electronic switches which are independently triggered by a firing circuit.

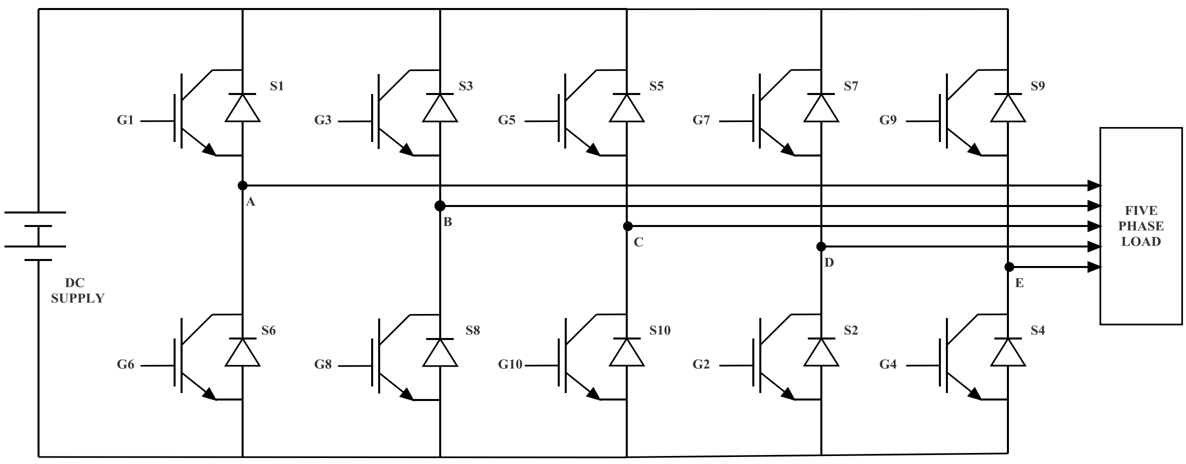

Figure 4.2: Circuit Diagram of a five phase VSI

From the figure 4.2, we can observe the ten switches numbered S_1, S_2,..., S_{10}. As a full cycle is of 360° duration and there are 5 legs, there are ten steps with each step in a five phase VSI of 36° duration. Each switch conduct for a duration of 180° and remain off for the other half. The switch in a leg is switched alternately at an interval of 180° and each switched is triggered 36° after the switch of the preceding index is triggered. The pulse waveform for the five phase VSI is shown in figure 4.3.

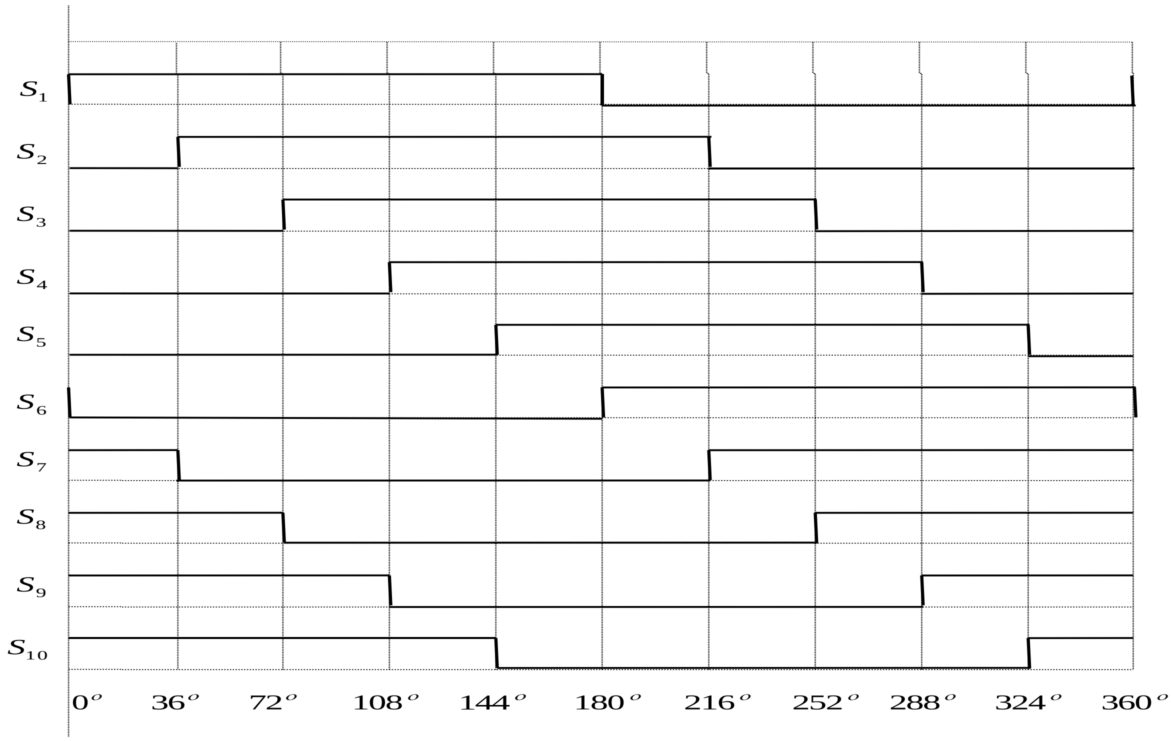

Figure 4.3: Switching pulse waveforms in a five phase VSI

As we can see from the figure 4.3 there are 10 steps along the angle axis. In each step, a set of five switches are on and the remaining are off. The switches which are on during each step is as follows:

$0° \ to \ 36°$: $S_7, S_8, S_9, S_{10}, S_1$

$36° \ to \ 72°$: $S_8, S_9, S_{10}, S_1, S_2$

$72° \ to \ 108°$: $S_9, S_{10}, S_1, S_2, S_3$

$108° \ to \ 144°$: $S_{10}, S_1, S_2, S_3, S_4$

$144° \ to \ 180°$: S_1, S_2, S_3, S_4, S_5

$180° \ to \ 216°$: S_2, S_3, S_4, S_5, S_6

$216° \ to \ 252°$: S_3, S_4, S_5, S_6, S_7

$252° \ to \ 288°$: S_4, S_5, S_6, S_7, S_8

$288° \ to \ 324°$: S_5, S_6, S_7, S_8, S_9

$324° \ to \ 360°$: $S_6, S_7, S_8, S_9, S_{10}$

Assuming equal impedence in each phase, and using simple voltage divider rule, we can find out the phase voltages. The waveform for the phase voltages in a five phase VSI is shown in figure 4.4.

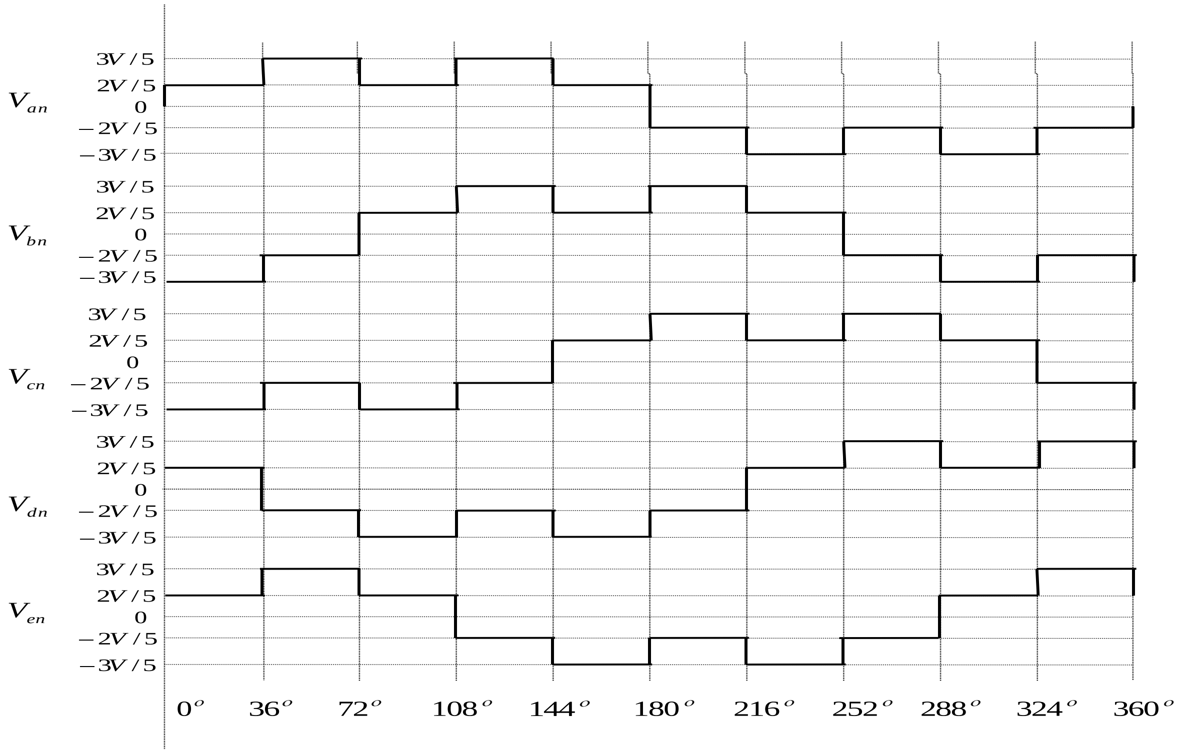

Figure 4.4: Phase Voltage waveforms in a five phase VSI

We can also represent the phase voltages in matrix form as

$$\begin{bmatrix} V_{an} \\ V_{bn} \\ V_{cn} \\ V_{dsn} \\ V_{en} \end{bmatrix} = \frac{V_{dc}}{5} \begin{bmatrix} 4 & -1 & -1 & -1 & -1 \\ -1 & 4 & -1 & -1 & -1 \\ -1 & -1 & 4 & -1 & -1 \\ -1 & -1 & -1 & 4 & -1 \\ -1 & -1 & -1 & -1 & 4 \end{bmatrix} \begin{bmatrix} S_a \\ S_b \\ S_c \\ S_d \\ S_e \end{bmatrix} \quad \cdots\cdots\cdots (4.21)$$

Where, S_a, S_b, S_c, S_d, S_e are the states of the five legs of the VSI. State 1 indicates that the upper switch is conducting whereas state 0 indicates that the lower switch is conducting.

For example, during $0°\ to\ 36°$ upper switches of phases a, d & e conduct whereas lower switches of phase b & c conduct. So, the states are $S_a = 1, S_b = 0, S_c = 0, S_d = 1, S_e = 1$.

Thus we have [21],

$$\begin{bmatrix} V_{an} \\ V_{bn} \\ V_{cn} \\ V_{dsn} \\ V_{en} \end{bmatrix} = \frac{V_{dc}}{5} \begin{bmatrix} 4 & -1 & -1 & -1 & -1 \\ -1 & 4 & -1 & -1 & -1 \\ -1 & -1 & 4 & -1 & -1 \\ -1 & -1 & -1 & 4 & -1 \\ -1 & -1 & -1 & -1 & 4 \end{bmatrix} \begin{bmatrix} 1 \\ 0 \\ 0 \\ 1 \\ 1 \end{bmatrix}$$

Hence,

$$\begin{bmatrix} V_{an} \\ V_{bn} \\ V_{cn} \\ V_{dn} \\ V_{en} \end{bmatrix} = \frac{V_{dc}}{5} \begin{bmatrix} +2 \\ -3 \\ -3 \\ +2 \\ +2 \end{bmatrix}$$

This result can be verified to be correct from the phase voltage waveform figure 4.4. Hence our matrix representation is correct.

4.4 State Vector in a five phase VSI

As there are five legs in a five phase VSI and each leg has two switch status, i.e. state 1 if upper switch is on or state 0 if lower switch is on. So in total there are $2^5 = 32$ switching vectors available in a five phase VSI. It is worth noting that the number of switching vectors in a three phase VSI was 8. As a result of these large number of switching vectors, a five phase VSI provides greater flexibility in choosing the optimum switching vector for DTC.

Now we have,

$$\vec{V_s} = \frac{2}{5}\left[V_{an} + V_{bn}e^{i2\pi/5} + V_{cn}e^{i4\pi/5} + V_{dn}e^{-i4\pi/5} + V_{en}e^{-i2\pi/5}\right]$$

We can put the values of the phase voltages obtained in each 32 states to generate the resultant voltage space vector.

Table 4.1: List of switching state in a five phase VSI

$\overline{V_s}$	V_{en}	V_{dn}	V_{cn}	V_{bn}	V_{an}	Switch status ($S_eS_dS_cS_bS_a$)	Magnitude (a=2V/5)	Angle(°)
V0	0	0	0	0	0	00000	0	-
V1	-V/5	-V/5	-V/5	-V/5	4V/5	00001	1.618 a	0
V2	-V/5	-V/5	-V/5	4V/5	-V/5	00010	1.618 a	72
V3	-2V/5	-2V/5	-2V/5	3V/5	3V/5	00011	1.618^2 a	36
V4	-V/5	-V/5	4V/5	-V/5	-V/5	00100	1.618 a	144
V5	-2V/5	-2V/5	3V/5	-2V/5	3V/5	00101	1 a	72
V6	-2V/5	-2V/5	3V/5	3V/5	-2V/5	00110	1.618^2 a	108
V7	-3V/5	-3V/5	2V/5	2V/5	2V/5	00111	1.618^2 a	72
V8	-V/5	4V/5	-V/5	-V/5	-V/5	01000	1.618 a	216
V9	-2V/5	3V/5	-2V/5	-2V/5	3V/5	01001	1 a	288
V10	-2V/5	3V/5	-2V/5	3V/5	-2V/5	01010	1 a	144
V11	-3V/5	2V/5	-3V/5	2V/5	2V/5	01011	1 a	36
V12	-2V/5	3V/5	3V/5	-2V/5	-2V/5	01100	1.618^2 a	180
V13	-3V/5	2V/5	2V/5	-3V/5	2V/5	01101	1 a	180
V14	-3V/5	2V/5	2V/5	2V/5	-3V/5	01110	1.618^2 a	144
V15	-4V/5	V/5	V/5	V/5	V/5	01111	1.618 a	108
V16	4V/5	-V/5	-V/5	-V/5	-V/5	10000	1.618 a	288
V17	3V/5	-2V/5	-2V/5	-2V/5	3V/5	10001	1 a	324
V18	3V/5	-2V/5	-2V/5	3V/5	-2V/5	10010	1.618^2 a	0
V19	2V/5	-3V/5	-3V/5	2V/5	2V/5	10011	1.618^2 a	0
V20	3V/5	-2V/5	3V/5	-2V/5	-2V/5	10100	1 a	216
V21	2V/5	-3V/5	2V/5	-3V/5	2V/5	10101	1 a	324
V22	2V/5	-3V/5	2V/5	2V/5	-3V/5	10110	1 a	108
V23	V/5	-4V/5	V/5	V/5	V/5	10111	1.618 a	36
V24	3V/5	3V/5	-2V/5	-2V/5	-2V/5	11000	1.618^2 a	252
V25	2V/5	2V/5	-3V/5	-3V/5	2V/5	11001	1.618^2 a	288
V26	2V/5	2V/5	-3V/5	2V/5	-3V/5	11010	1 a	252
V27	V/5	V/5	-4V/5	V/5	V/5	11011	1.618 a	324
V28	2V/5	2V/5	2V/5	-3V/5	-3V/5	11100	1.618^2 a	216
V29	V/5	V/5	V/5	-4V/5	V/5	11101	1.618 a	252
V30	V/5	V/5	V/5	V/5	-4V/5	11110	1.618 a	180
V31	0	0	0	0	0	11111	0	-

Example:

1. Let us consider the case of V1:

   Here, $(S_a = 1, S_b = 0, S_c = 0, S_d = 0, S_e = 0)$

   So,

   $V_{an} = \frac{4V}{5}, V_{bn} = \frac{-V}{5}, V_{cn} = \frac{-V}{5}, V_{an} = \frac{-V}{5}, V_{an} = \frac{-V}{5}$

   Putting this values in the complex equation we have

   $\overrightarrow{V1} = \frac{2V}{5}\left[\frac{4}{5} - \frac{1}{5}e^{i2\pi/5} - \frac{1}{5}e^{i4\pi/5} - \frac{1}{5}e^{-i4\pi/5} - \frac{1}{5}e^{-i2\pi/5}\right]$

   $\overrightarrow{V1} = 1.618 * \frac{2V}{5}\angle 0°$

2. Let us consider the case of V3:

   Here, $(S_a = 1, S_b = 1, S_c = 0, S_d = 0, S_e = 0)$

   So,

   $V_{an} = \frac{3V}{5}, V_{bn} = \frac{3V}{5}, V_{cn} = \frac{-2V}{5}, V_{an} = \frac{-2V}{5}, V_{an} = \frac{-2V}{5}$

   Putting this values in the complex equation we have

   $\overrightarrow{V3} = \frac{2V}{5}\left[\frac{3}{5} + \frac{3}{5}e^{i2\pi/5} - \frac{2}{5}e^{i4\pi/5} - \frac{2}{5}e^{-i4\pi/5} - \frac{2}{5}e^{-i2\pi/5}\right]$

   $\overrightarrow{V3} = 1.618^2 * \frac{2V}{5}\angle 36°$

3. Let us consider the case of V5:

   Here, $(S_a = 1, S_b = 0, S_c = 1, S_d = 0, S_e = 0)$

   So,

   $V_{an} = \frac{3V}{5}, V_{bn} = \frac{-2V}{5}, V_{cn} = \frac{3V}{5}, V_{an} = \frac{-2V}{5}, V_{an} = \frac{-2V}{5}$

   Putting this values in the complex equation we have

   $\overrightarrow{V5} = \frac{2V}{5}\left[\frac{3}{5} - \frac{2}{5}e^{i2\pi/5} + \frac{3}{5}e^{i4\pi/5} - \frac{2}{5}e^{-i4\pi/5} - \frac{2}{5}e^{-i2\pi/5}\right]$

   $\overrightarrow{V5} = 1 * \frac{2V}{5}\angle 72°$

It is observed that vectors $\overrightarrow{V0}\ and\ \overrightarrow{V31}$ have magnitude 0 because in these two cases the circuit is open. Thus these are called null vectors.

Rest of the vectors can be divided into three groups depending on their magnitude

- Inner group $(1 * \frac{2V}{5})$: V18,V11,V5,V22,V10,V13,V20,V26,V9,V21
- Middle group $(1.618 * \frac{2V}{5})$: V1,V23,V2,V15,V4,V30,V8,V29,V16,V27
- Outer group $(1.618^2 * \frac{2V}{5})$: V19,V3,V7,V6,V14,V12,V28,V24,V25,V17

Thus the magnitude of the vectors are in the ratio 1: 1.618: 1.618^2 from inner to outer group [12]. The significance of these three groups is that they give us the luxury to choose the vector according to our requirement. If we want a large change in the result, we have to use the outer group vectors as they have the highest magnitude. Similarly, if we want very minute change in the output, we have to use the inner group vectors as they have the least magnitude. The middle group of vectors are generally used for intermediary changes. Thus this ensures more accuracy in the result and hence make the ripples small. This is the main reason why DTC in multi-phase machines produce smaller torque ripples than their three phase counterparts.

4.5 Look up table for five phase DTC

Figure 4.5 shows the space representation of the 32 switching vectors. It can be clearly seen that there are three set of vectors with different magnitudes. The angle between each neighboring vector is 36°.

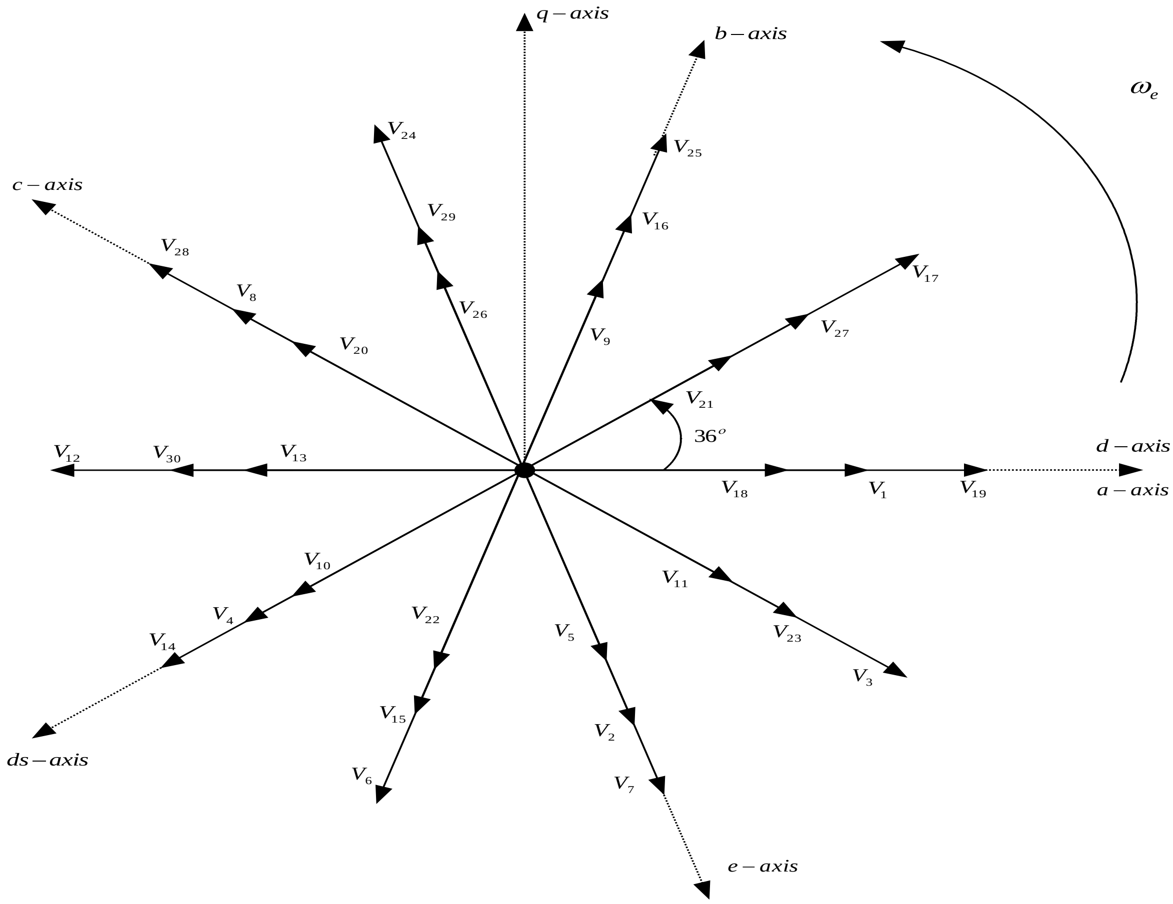

Figure 4.5: State vector diagram in a five phase VSI

The entire space of $360°$ is divided into 10 sectors of $36°$ for proper location of the stator flux linkage vector. The distribution of sectors is shown in figure 4.6. Here S_1, S_2,… S_{10} represent the ten sectors.

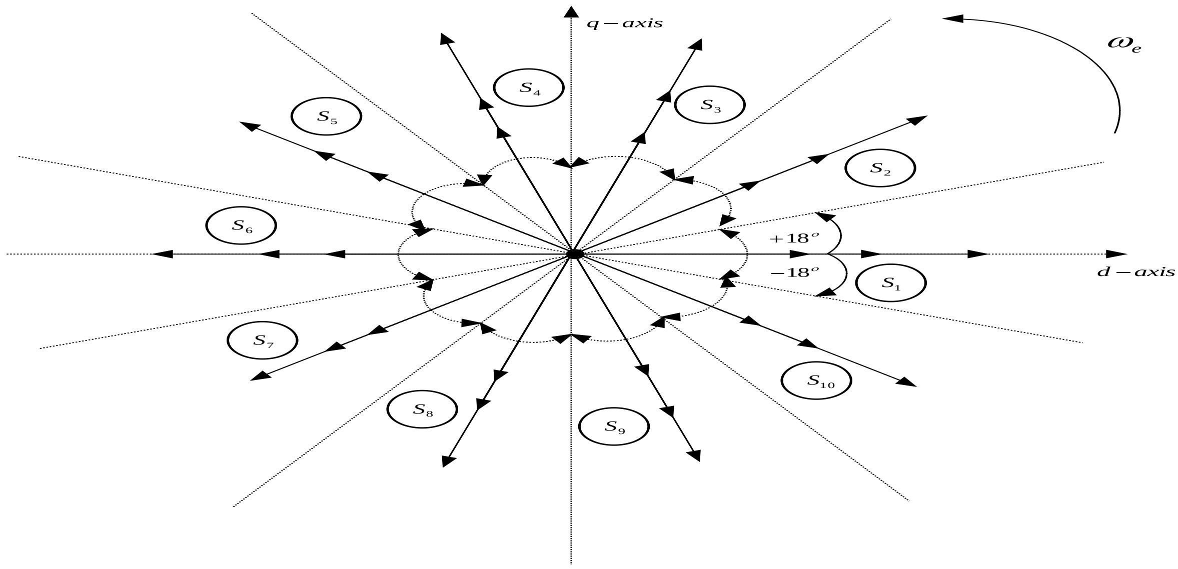

Figure 4.6: Distribution of sectors in the state vector diagram in a five phase VSI

If we assume that the stator flux is in sector 1, with the rotor flux along d-axis, the table 4.2 shows the effect of various state vectors of outer group on torque and flux. Here the number of arrows indicate the intensity of change. For example, ↑↑↑ indicates large increase, ↑↑ indicates intermediate increase and ↑ indicate small increase. Similarly, it can be inferred for decrease also.

Table 4.2: Effect of outer group vectors on torque and flux

State vector, $\bar{V}$	Effect on flux, ψ_s	Effect on Torque, T_e
V19	↑↑↑	-
V3	↑↑	↓↓
V7	↑	↓↓↓
V6	↓	↓↓↓
V14	↓↓	↓↓
V12	↓↓↓	-
V28	↓↓	↑↑
V24	↓	↑↑↑
V25	↑	↑↑↑
V17	↑↑	↑↑

The effect of the other two groups are also similar but due to lesser magnitude the effect of the vectors in the resultant is lesser than the outer group. The figure 4.7 shows the difference in the effect of the three vector groups.

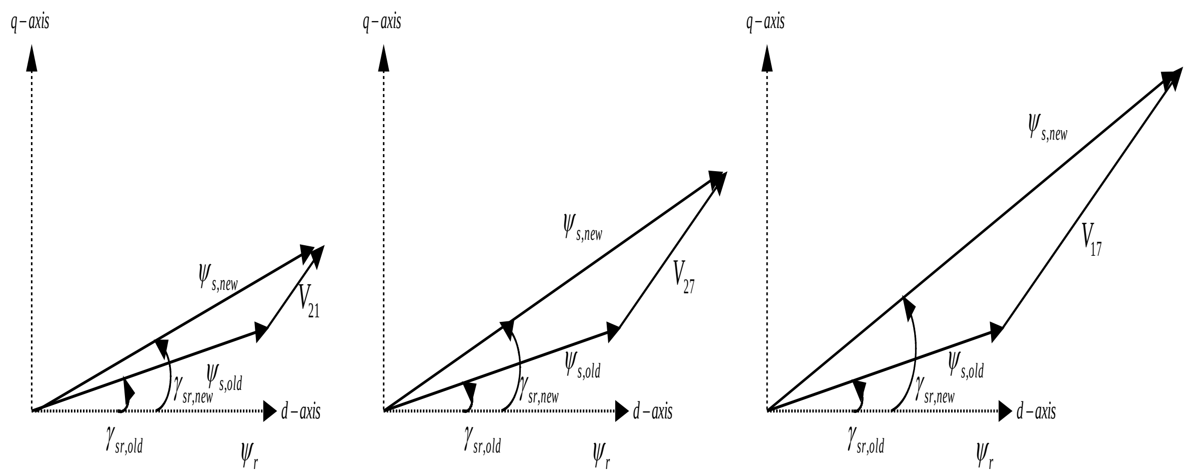

Figure 4.7: Comparison of effect of vectors of different vector groups

The inner vector V_{21} has a very small change on the resultant magnitude and angle. The middle vector V_{27} has relatively higher angle change and greater resultant magnitude than the inner group. However, we can see that with the outer voltage vector V_{17} the change is large. Hence for large changes the outer group is preferred whereas for minute changes inner group. For all intermediate purposes the middle group is preferred.

In the simulation, a two level hysteresis controller is used for the flux linkage and a seven levelled hysteresis controller is used for the torque. The higher level of hysteresis control gives us more flexibility in choosing the optimum switching vector. This however, increases the complexity of the program. On the basis of the effect of various switching vectors on the torque and flux of the machine, a look up table has been prepared here. In this simulation, only the middle vectors are used for the sake of simplicity. One can use any combination of vectors according to the need. The look up table used in the simulation is given in table 4.3.

Table 4.3: Look up Table for DTC in a five phase Induction Motor

Flux Error	Torque Error	Sector 1	Sector 2	Sector 3	Sector 4	Sector 5	Sector 6	Sector 7	Sector 8	Sector 9	Sector 10
	-3(↓↓↓)	4	15	2	23	1	27	16	29	8	30
	-2(↓↓)	22	5	11	18	21	9	26	20	13	10
	-1(↓)	10	22	5	11	18	21	9	26	20	13
-1(↓)	0	13	10	5	5	11	18	21	9	26	20
	1(↑)	20	13	10	22	5	11	18	21	9	26
	2(↑↑)	26	20	13	10	22	5	11	18	21	9
	3(↑↑↑)	8	30	4	15	2	23	1	27	16	29
	-3(↓↓↓)	23	1	27	16	29	8	30	4	15	2
	-2(↓↓)	5	11	18	21	9	26	20	13	10	22
	-1(↓)	11	18	21	9	26	20	13	10	22	5
1(↑)	0	18	21	9	26	20	13	10	5	5	11
	1(↑)	21	9	26	20	13	10	22	5	11	18
	2(↑↑)	9	26	20	13	10	22	5	11	18	21
	3(↑↑↑)	27	16	29	8	30	4	15	2	23	1

4.6 Simulink Model

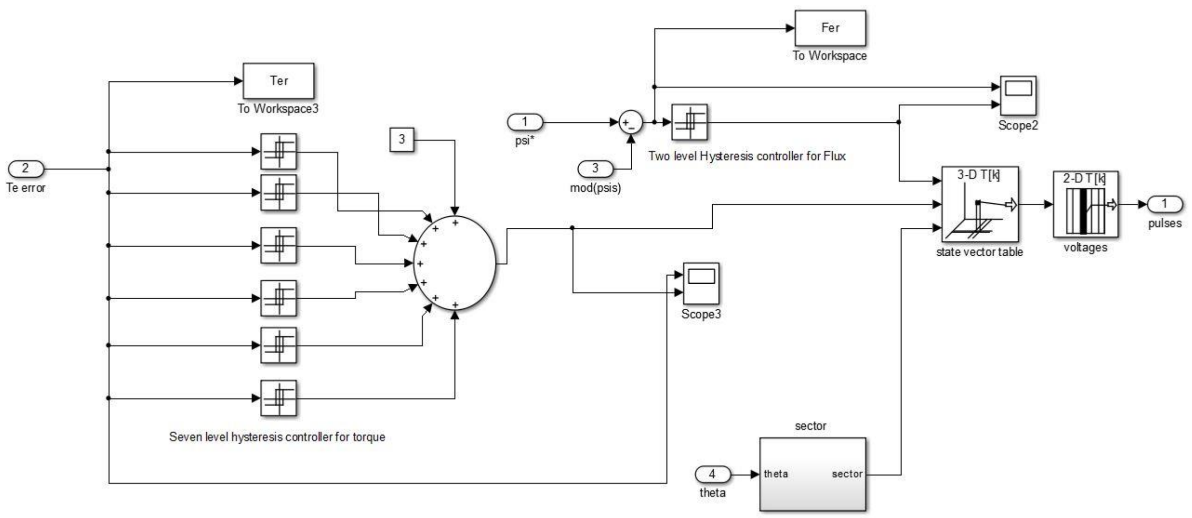

Figure 4.8: Simulink Model of DTC block in a five phase induction motor

4.7 Summary

In this chapter we obtained the transformation matrix from five phase variables to two phase mutually perpendicular quantities. We also observed that the phase equivalent model of the five phase induction motor was identical to the three phase machine and hence all the phase equations were same. The thirty-two switching vectors were obtained from the five phase VSI and after calculating their magnitude and phase from the state vector equation, the state vector diagram was obtained. From the state vector diagram it was observed that the thirty active vectors of the five phase VSI were divided into three vector groups of different magnitude and each group contained ten vectors. The impact of each switching vector on the torque and flux change was observed and subsequently a look up table was designed to choose the optimum switching state depending on the torque error, flux error and the sector information.

Chapter 5

Results and Conclusion

Using the modelling equations, both three phase and five phase induction motors are modelled and various simulations are performed. Direct torque Control is simulated for both three phase and five phase machines with identical machine parameters. The machine parameters are given in table 5.1. The stator flux linkage is kept constant at 0.95 V-s. The simulations are performed with fundamental sample time of 50 μs, i.e. the sampling frequency is 20KHz.

Table 5.1: Machine Parameters

Parameter	Value
Power	3Hp (2238W)
Rated Frequency	50Hz
Rated Voltage	440V
Number of Poles	4
Rated Speed	1500 rpm or 157 rad/s
Stator resistance in ohm	1.77
Stator leakage reactance (H)	13.93e-3
Rotor resistance in ohm	1.34
Rotor leakage reactance (H)	12.12e-3
Mutual Inductance (H)	369e-3
Moment of inertia (Kgm^2)	0.025

5.1 Waveforms of three phase DTC

1. Torque Response

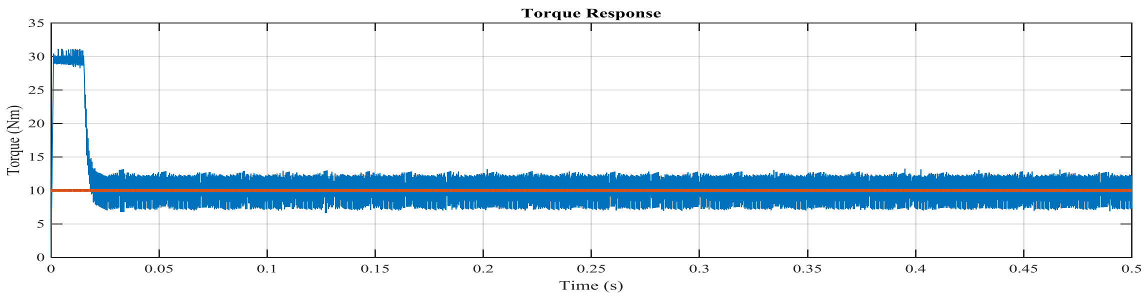

Figure 5.1

2. Torque Ripple

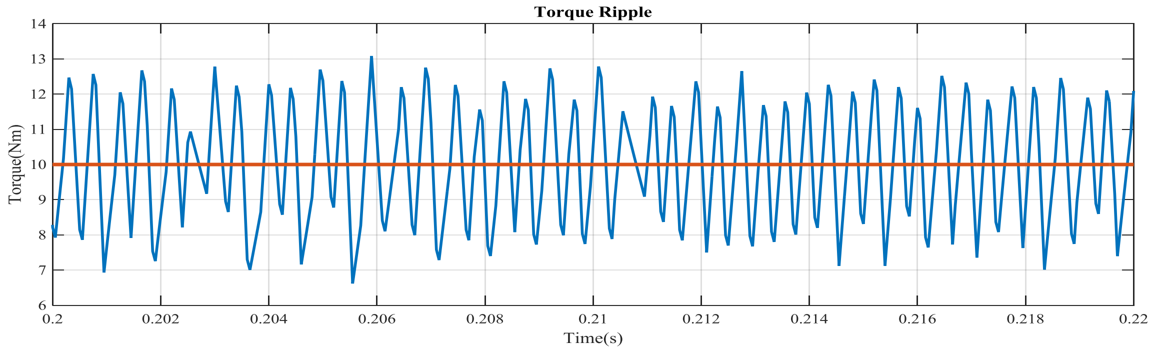

Figure 5.2

3. Stator current i_d and i_q

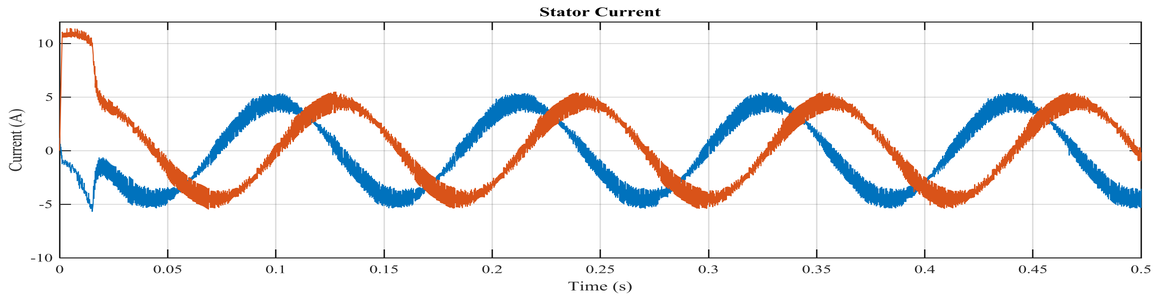

Figure 5.3

4. Flux Trajectory

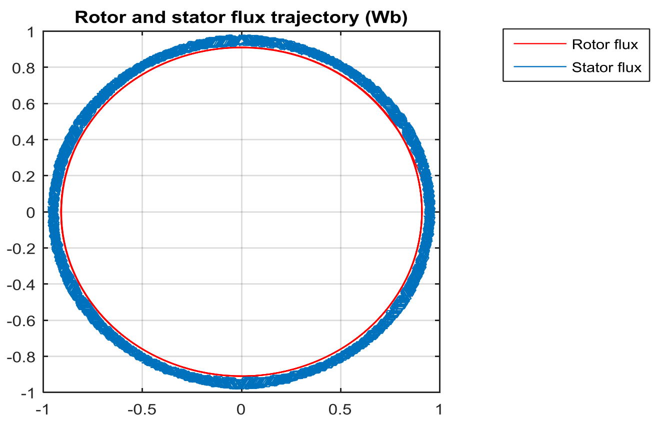

Figure 5.4

5. Torque Response to varying load

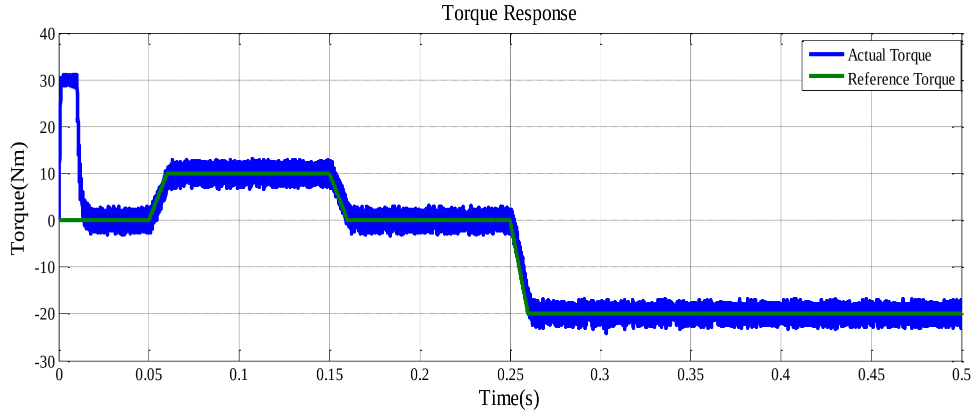

Figure 5.5

5.2 Waveforms of five phase DTC

1. Torque Response

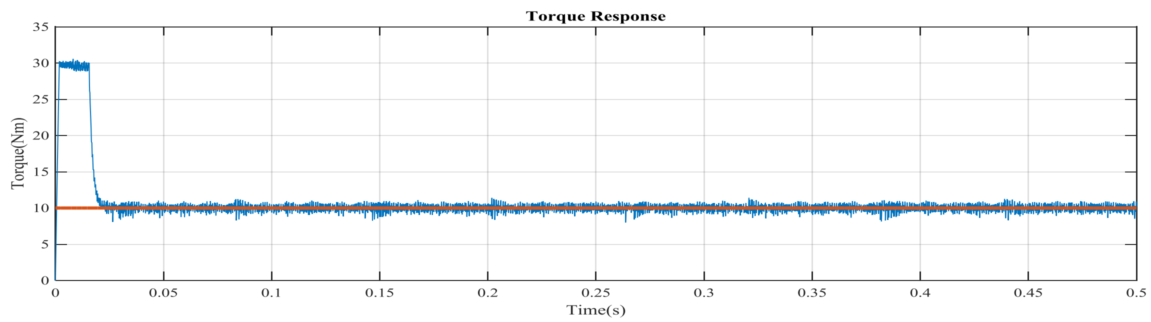

Figure 5.6

2. Torque Ripple

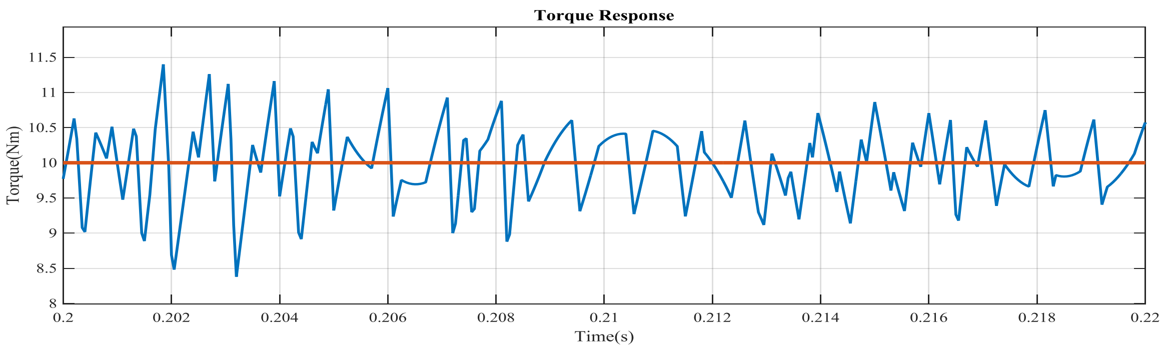

Figure 5.7

3. Stator current i_d and i_q

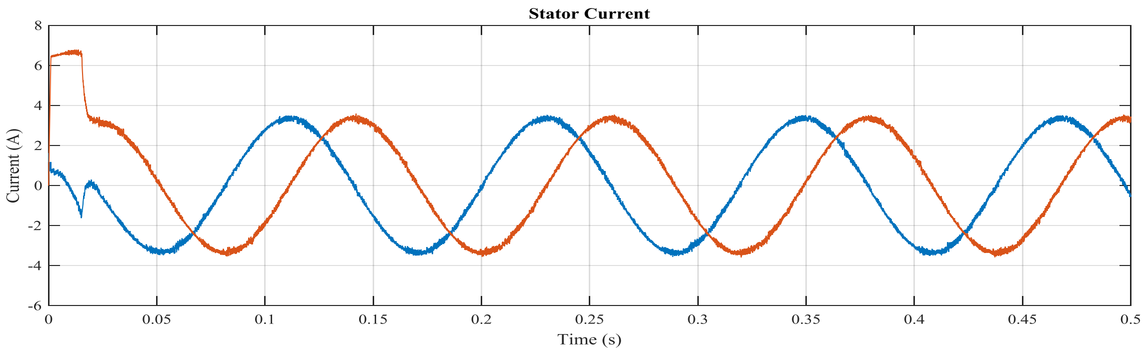

Figure 5.8

4. Flux Trajectory

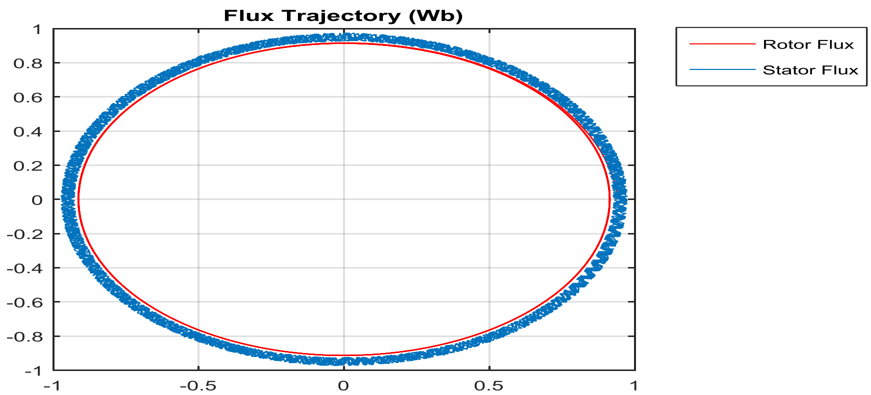

Figure 5.9

5. Torque Response to varying load

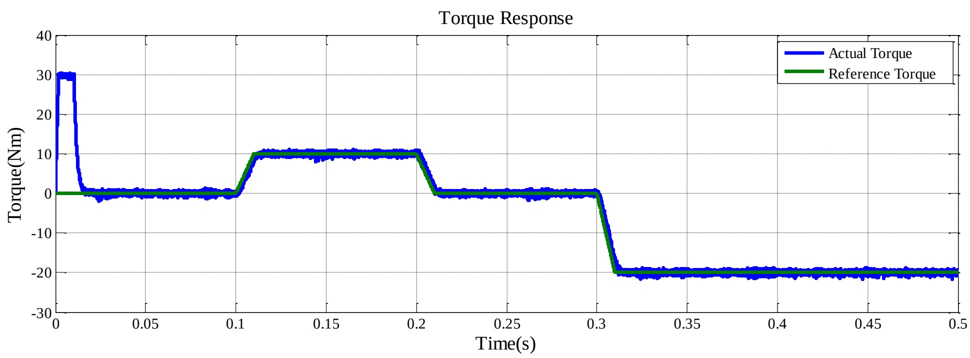

Figure 5.10

5.3 Comparison between three phase and five phase DTC

1. Torque response

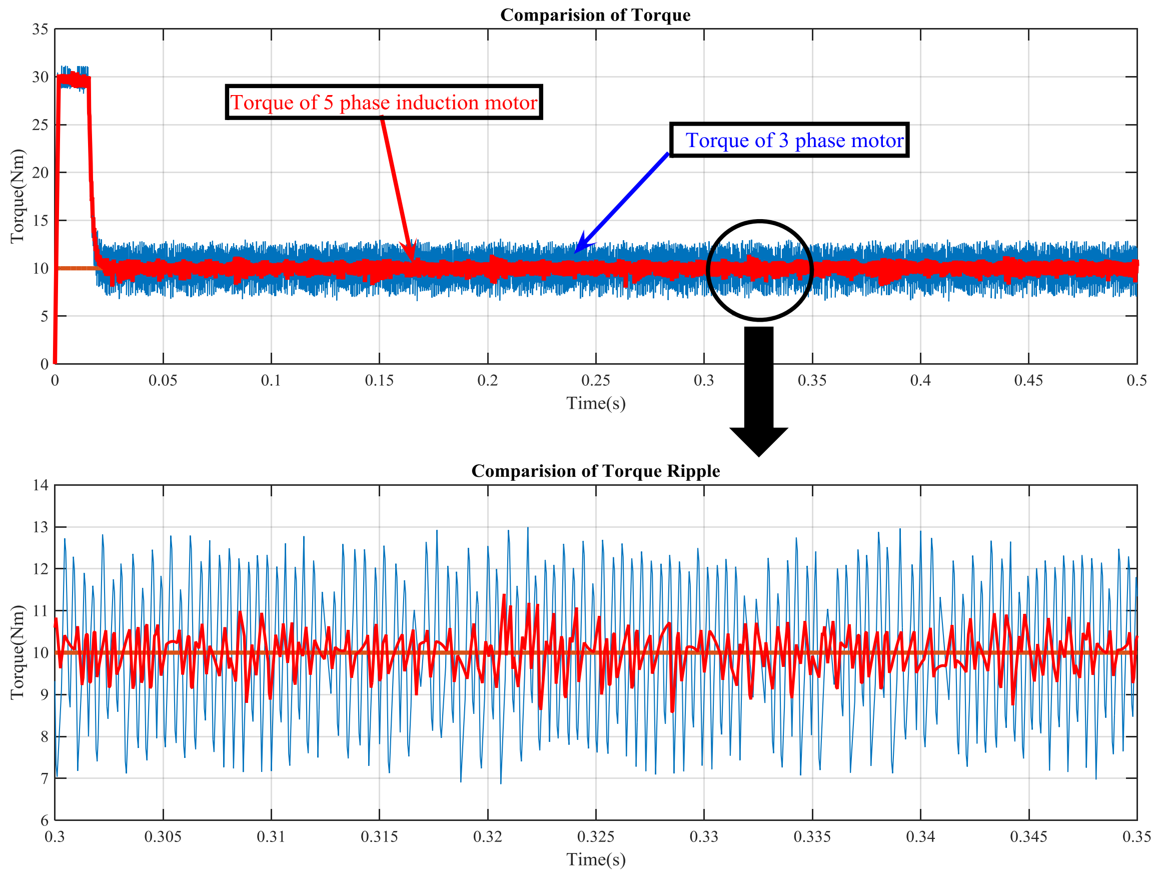

Figure 5.11

2. Torque Response to varying load

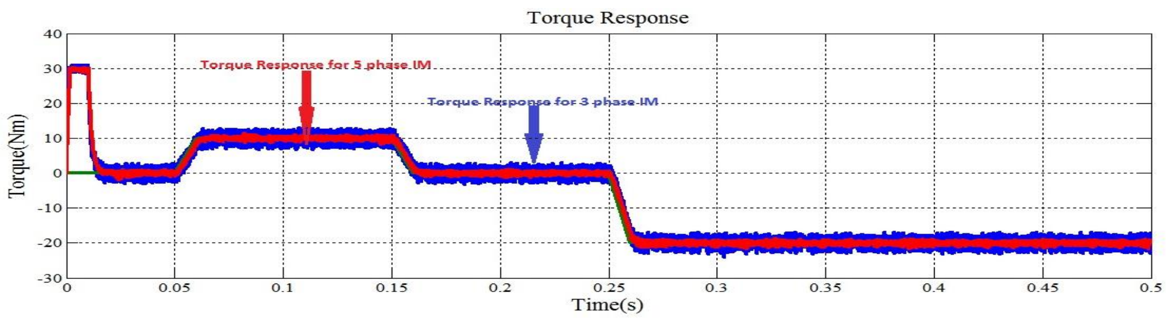

Figure 5.12

3. Stator Flux Trajectory

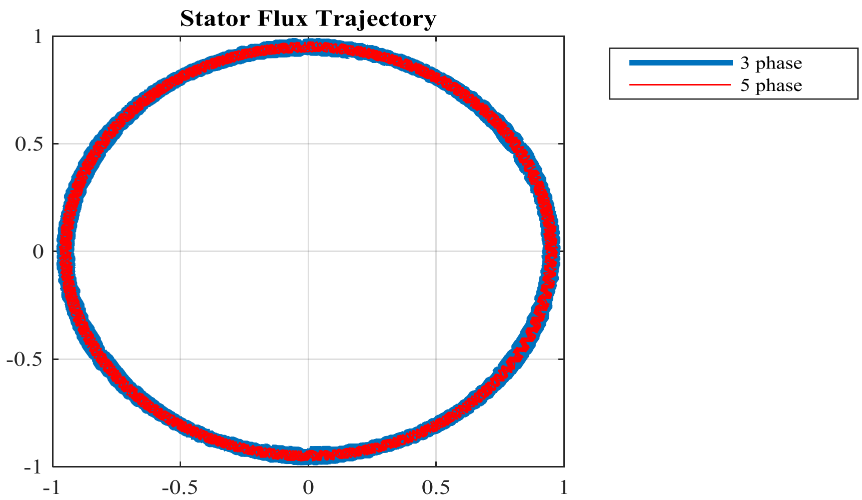

Figure 5.13

5.4 Results and Conclusion

From the waveforms we observe that for the same parameters,

- Five phase motor has a torque ripple of $\pm 1.5Nm$ whereas a three phase motor has a ripple of $\pm 3Nm$.
- Stator flux trajectory of five phase motor is smoother and narrower than the three phase motor which indicates lower flux ripples.
- Ripples in the stator current is also significantly lower in the five phase machine than the three phase motor.

Thus DTC of five phase induction machine can result in a more accurate control of stator flux and torque. Hence we can achieve very accurate and precise dynamic torque response.

Chapter 6

Summary

6.1 Summary of the work

The objective of the project was to validate the fact that DTC of multi-phase induction machines produce lower torque ripples than a three phase machine. For this both three phase and five phase machine were modelled using Simulink. Eight switching state vectors were obtained from the complex representation of the three phase VSI, whereas, thirty-two switching state vectors were obtained from the five phase VSI. The transformation matrix in a five phase induction machine was obtained by vector resolution technique. The effect of each switching vector on the flux and torque output of the machine was analyzed and an optimum look up table was prepared for both the type of machines. The entire DTC process was simulated for both the machines using Simulink. The torque output waveforms, the current waveforms and the flux trajectory waveforms were obtained from both the simulations. It was observed that the torque ripple in the five phase machine was reduced by 50% as compared to that of the three phase machine. Also the flux trajectory was narrower in the five phase machine, indicating that the flux ripples were less. Also the stator current waveforms had less ripples in case of the five phase machine. Thus the objective of the project was achieved.

6.2 Scope for future work

1. Hardware implementation of the work can be done to experimentally verify the conclusion.
2. Advanced DTC control techniques like the DTC-SVM and Fuzzy logic approach can be tried to validate the result.
3. The other features of multi-phase machines such as higher fault tolerance and better tolerance for harmonic components can be studied and tried to validate experimentally.
4. Vector control techniques can be simulated for a multi-phase machine and the results can be compared with that of a three phase machine.

REFERENCES

[1] I. Takahashi and T. Noguchi, “A new quick-response and high-efficient control strategy of an induction motor” *IEEE Trans. Ind. Applicat.*, vol. IA-22,pp. 820-827, Sept./Oct. 1986.

[2] M. Depenbrock, “Direct self-control of inverter-fed induction machine,” *IEEE Trans. Power Electrinics,* vol.3,pp.420-429, Oct 1988.

[3] T.G. Habetler, F. Profumo, M. Pastorelli and L.M. Tolbert, “Direct Torque control of induction machines using space vector modulation”, *IEEE Trans. Ind. Applicat.*, vol. 28,pp. 1043-1045,Sept./Oct. 1992

[4] S.Mir and M.E. Elbuluk, “Precision control in inverter-fed induction machines using fuzzy logic”, in *PROC. IEEE Power Electronics Soc. Conf.*, pp. 396-401,1995

[5] J. Chen and Y.Li, “Virtual vectors based predictive control of torque and flux of induction motor and speed sensorless drives”, in *Conf. Rec. IEEE-IAS Annual Meeting,* pp. 2606-2613,1999.

[6] D.Telford, M.W. Dunnigan and B.W. Williams, “A novel torque-ripple reduction strategy for direct torque control”, *IEEE Trans. Ind. Electronics*, vol.48, pp. 867-870, Aug. 2001.

[7] J.K. Kang and S.K. Sul, “Analysis and prediction of inverter switching frequency in direct torque control of induction machine based on hysteresis band and machine parameters”, *IEEE Trans. Ind. Application*, vol. 35, pp. 545-553, Sept./Oct 1999.

[8] S.K. Lin and C.H. Fang, “Sliding-Mode Direct Torque Control of an Induction Motor”, *IEEE Annual Conf. Ind. Electronics,* IECON,vol.3, pp. 2171-2177, 2001.

[9] H. Yourui and T. Chaoli, “Direct Torque Control of Induction Motor by use of Neural Network”, *IEEE International conf. on Electrical Machines and systems*, vol. 3, pp. 2415-2417, 2005

[10] M. Dybkowski and K. Szabat, “Direct Torque Control of Induction Motor Drive System with Adaptive Sliding-Mode Neuro-Fuzzy Compensator”, *IEEE International conf. on Industrial Technology,* pg. 714-719, 2015

[11] I.M. Alsofyani and Idris, “Simple Flux Regulation for Improving State Estimation at very Low and Zero speed sensorless Direct Torque Control of an induction motor”, *IEEE Transactions on Power Electronics*, vol. 31, pp. 865-872, April 2016

[12] H. Toliyat, T.A. Lipo and J. White, “Analysis of a Concentrated Winding Induction Machine for Adjustable Speed Drive Aplications”, *IEEE Trans. On Energy Conversion*, vol. 6, pp. 684-692, Dec 1991.

[13] E.E. Ward and H. Harer, “Preliminary Investigation of an Inverter-Fed 5-Phase Induction Motor”, *Proc. IEE,* vol. 116, pp. 980-984, 1969

[14] E.A. Klingshim, “High Phase Order Induction Motors- Part 1 and II”, *IEEE Trans. Power Appl.*, vol. PAS-102, pp. 775-780, Jan 1983

[15] K.N. Pavithran, R. Parimelalagan and M.R. Krishnamurthy, “Studies on Inverter- Fed Five Phase Induction Motor Drive”, *IEEE Power Elec.*, vol. 3, pp. 224-235, Apr. 1988

[16] H.A. Toliyat and H. Xu, “A novel direct torque control (DTC) method for five-phase induction machines”, *Proceedings of the IEEE Applied Power Electronics Conference*, vol.1, pp. 456-463, Sept. 2001

[17] S. Lu, K. Corzine, “Direct Torque Control of Five-Phase Induction Motor using space vector modulation with Harmonics Elimination and Optimal switching sequence”, *IEEE Annual conf. on applied power electronics,* 2006

[18] B.S. Khaldi, H.Abu-Rub etal., “Sensorless Direct Torque Control of Five-Phase Induction Motor Drives”, *IEEE Annual conf. on industrial electronics,* pg. 3501-3506, *2011*

[19] J.A. Riveros, M.J. Duran, F. Barrero, S. Toral, “Direct Torque Control for Five-Phase Induction Motor Drives with Reduced Common mode voltage”, *IEEE Annual conf. on industrial electronics,* pp. 3616- 3621, 2012

[20] B.K. Bose, “Power Electronics and Variable Frequency Drives”, *IEEE Press,* 1997

[21] H. Guzman, J.A. Riveros etal., “Modelling of a Five-Phase Induction Motor Drive with a faulty Phase”, *Interantional Power Electronics and Motion Control Conference*, pp. LS1c.3-1 - LS1c.3-6, 2012

[22] E. Levi, R. Bojoi, etal., “Multiphase induction motor drives- a technology status review”, *IET Industrial Power Applications*, vol. 1, pp. 489-516, 2007